UNIVERSITY OF NAIROBI

PREDICTABILITY OF PRECIPITATION ON MEDIUM RANGE TIMESCALE OVER THE GREATER HORN OF AFRICA REGION USING THE SUPERENSEMBLE TECHNIQUE

BY

KIPKOGEI OLIVER
I56/83634/2012

A DISSERTATION SUBMITTED IN PARTIAL FULFILLMENT OF THE REQUIREMENTS FOR THE AWARD OF THE DEGREE OF MASTER OF SCIENCE IN METEOROLOGY IN THE UNIVERSITY OF NAIROBI

2014

DECLARATION

This dissertation is my original work and has not been presented for examination in any other University.

Oliver Kipkogei

Signature…….....

Date……

This dissertation has been submitted for examination with our approval as University Supervisors.

Prof. Laban Ogallo

Signature…….

Date ……

Dr. Franklin Opijah

Signature……

Date……

Dr. Joseph Mutemi

Signature……

Date……

DEDICATION

I dedicate this research to my late grandfather Mr. Cheruiyot Kemei and my mother Jane Kemei who built in me the spirit of determination to achieve my vision. To my fiancée, Tabitha; I remember talking endlessly about the superensemble codes yet you still had the patience to lend me an ear. You still loved me when I talked about Zanzibar despite my failure to plan a vacation that actually takes you there…yet. Virtue, itself, smiles at your example of patience.

ABSTRACT

Superensemble forecasts derived from a suite of multiple models are a useful tool in rainfall prediction, in which the models from THORPEX Interactive Grand Global Ensemble (TIGGE) operational suite are employed.

The overall objective of this study was to assess the predictability of precipitation on medium range timescale over the Greater Horn of Africa region using the superensemble technique. Forecast datasets from TIGGE and rain rates from Tropical Rainfall Measuring Mission (TRMM) were used to construct a multimodel Superensemble precipitation forecast for the period 20 to 29 November, 2013. Previous 450 days of Multimodel forecast data of 2008 to 2012 during the months of October, November and December were used to train the model and calculate statistical weights.

Standard metrics for forecast validations that included the Root Mean Square Error (RMSE), Equitable Threat Score (ETS), Spatial Correlation (SC) and Bias were used. Four individual runs were undertaken to ensure that the results were stable. In all runs, it was noted that the multimodel superensemble carried a consistent higher skill in terms of SC and RMSE as compared with that of the individual member models in the suite. The superensemble ETS and bias scores for all forecasts carried the best scores close to 1.0.
Skill forecasts of precipitation clearly demonstrate that it is possible to obtain higher skills for precipitation forecasts for Days 1 through 10 of forecasts from the use of the multimodel superensemble as compared to the best model in the suite. The higher skills of the multimodel superensemble make it a very useful tool for prediction and early warning of the risks associated with extreme weather and climate events.

ACKNOWLEDGMENTS

This research study was supported by the IGAD Climate Prediction and Applications Centre (ICPAC). I sincerely thank Professor Laban A. Ogallo, Director ICPAC, for his mentorship and also for granting me an opportunity to undertake my research at the Florida State University. I feel indebted to my direct supervisor, Professor T.N. Krishnamurti for his guidance throughout the research period. I am grateful to Amit Bardhwaj and Vinay Kumar for helping me understand the Superensemble code and tirelessly working with me throughout my research. Without their assistance, these words may never have been put on paper. Words alone cannot describe how grateful I am. Special thanks also go to my Supervisors Dr. Frankline Opijah and Dr. Joseph Mutemi.

I would also like to express my appreciation to the collaboration between the University of Nairobi and IGAD Climate Prediction and Applications Centre (ICPAC) that granted me the opportunity to pursue a degree in Master of Science (Meteorology) through an academic scholarship.

Finally I acknowledge my colleagues at ICPAC for their academic and moral support which has been invaluable.

TABLE OF CONTENTS

LIST OF FIGURES

LIST OF TABLES

LIST OF ACRONYMS AND THEIR MEANING

AGCMs	Atmospheric General Circulation Models
BMRC	Bureau of Meteorology Research Centre
CERES	Clouds and the Earths Radiant Energy
CMC	Canadian Meteorological Centre
DMI	Indian Ocean Dipole Mode
DMSP	Defense Meteorology Space Program
EAC	East African Community
ECHAM	European Centre Hamburg Model
ECMWF	European Centre for Medium range Weather Forecasts
ENSO	El Niño Southern Oscillations
ETS	Equitable Threat Score
FAR	False Alarm Ratio
FNMOC	Fleet Numerical Meteorology and Oceanography Centre
FSU	Florida State University
FSUGSM	Florida State University Global Spectral Model
FSUSE	Florida State University Superensemble
GFDL	Geophysical Fluid Dynamics Laboratory
GFS	Global Forecasting System
GHA	Greater Horn of Africa
GPCs	Global Producing Centers

HDF	Hierarchical Data Format
HSS	Heidke Skill Score
ICPAC	IGAD Climate Prediction and Applications Centre
IMD	India Meteorological Department
IRI	International Research Institute
ITCZ	Inter-Tropical Convergence Zone
JAXA	Japan Aerospace Exploration Agency
JMA	Japan Meteorological Agency
LIS	Lighting Imaging Sensor
MAM	March April May
MJO	Madden Julian Oscillation
MOS	Model Output Statistics
NASA	National Aeronautics and Space Agency
NCEP	National Center for Environmental Prediction
NESDIS/	National Environmental Satellite, Data, and Information Service
NH	Northern Hemisphere
NOAA	National Oceanic and Atmospheric Administration
NOGAPS	Navy Operational Global Atmospheric Prediction System
NWP	Numerical Weather Prediction
NWS	National Weather Service
PI	Physical Initialization

POD	Probability of Detection
PR	Precipitation Radar
QBO	Quasi Biennial Oscillation
QPEs	Quantitative Precipitation Estimates
RMSE	Root Mean Square Error
SE	Superensemble
SH	Southern Hemisphere
SSM/I	Special Sensor Microwave/Imager
SSM/I	Special Sensor Microwave/Imager
SVD	Singular Value Decomposition
TMI	TRMM Microwave Imager
TRMM	Tropical Rainfall Monitoring Mission
UKMO	United Kingdom Meteorological Office
VIRS	Visible Infrared Scanner

CHAPTER ONE

1.0 Introduction

This section provides a brief description on the background study, problem statement, study objectives, justification, hypothesis and area of the study.

1.1 Background Study

Understanding and predicting weather and climate system is a challenging problem of great scientific interest. Our growing understanding of interactions between the atmosphere, oceans, biosphere, cryosphere and land surface is revolutionizing the earth and atmospheric sciences. Owing to the complexity of interacting processes which constitute weather and climate, and the fact that weather affects man's welfare; mathematical models have been developed at the numerical laboratories for studying how the system operates and predictions. Various numerical models perform to various levels of skill at different areas due to differences in modeling specific concepts and specifics of formulating processes applied by different model developers.

The Superensemble technique was initially developed at Florida State University (FSU). It is a powerful post-processing method for the estimation of weather forecast parameters, reducing direct model output errors based on the availability of real time forecast outputs from various models. The uniqueness of this approach lies in model weighting methodology with uptake of performance from observations. Therefore, it differs from other ensemble prediction schemes (Krishnamurti *et al*., 1999; 2000a; 2000b; Chaves *et al.,* 2005).

The Superensemble (SE) technique is used to gather valuable predictive information from some of the best available weather model forecasts, and further, to combine that information to generate a forecast that has superior accuracy. A SE forecast is completely objective (Krishnamurti, 1999). Because of this, SE forecasts are ideal when weather forecasts must serve as inputs to other statistical models. Also of importance, the SE forecasts and their associated datasets form an objective basis for probabilistic forecasting. Probabilistic forecasts add value to decision making processes, particularly when examining risk associated with a weather hazard.

The Superensemble has higher forecast skills compared to that of the ensemble mean (Mishra *et al.,* 2007). The difference arises because the ensemble mean assigns a weight of 1 to all participating models and does not correct the bias of the models based on their past behavior. This results in the inclusion of some of the poorer models as well, thus the skill of the ensemble mean is degraded. The Superensemble is selective in assigning weights and the past history of performance of models has a major role compared to that of current forecasts by the multi-models. It assigns fractional or even negative weights and is very selective (Williford *et al*., 2003)

The Superensemble also performs better than the ensemble means of individual models whose bias has been removed (Krishnamurti and Kumar, 2012). The removal of bias of poorer models does not appear to bring them up to the levels of the best models, and assigning an equal weight to such models for the construction of the ensemble mean does not bring it to the level of the proposed Superensemble. The latter benefits from the geographically selective weights based on past performance (Krishnamurti, 1999).

It is important to note that the Superensemble is not a simple averaging technique. In many cases, its forecasts correctly lie outside the range of input model forecasts. In general, this process reduces the impact of initial errors in a forecast. Not only can an ensemble lead to a better forecast, it can also reveal how reliable a forecast is in judging from the spread of the different forecasts (Buizza, 1998).

Medium range forecasts of up to 10 days is one of the key priorities at IGAD Climate Prediction and Applications Centre (ICPAC) and regional National Meteorological and Hydrological Services (NMHSs) due to the significant impacts of weather and climate extremes such as floods and drought in the region. The major focus of this study is to investigate the predictability of precipitation on medium range timescale over the Greater Horn of Africa region using the superensemble technique

1.2 Problem Statement

There is increased need for improving accuracy of forecasts at all timescales in the region. Great strides have been achieved in meteorological research, forecasting and modeling. However, the existing forecast products fall short of the expectation, especially on the short to medium timescales. Skillful prediction in this range is thus a very important component in any operational weather and climate institution.

The increased demand for the service by the user community is necessitated by the fact that the social and economic well being in the Greater Horn of Africa region is dependent on rain-fed agriculture. Weather and climate extremes like floods and drought pose the greatest risk in the region's economy. The population is unable to absorb the shocks resulting from such events due to lack of information and resources. Accurate and timely forecasts on onset, intensity, distribution, and cessation should be attained.

Currently, the region relies mostly on the use of point station data as the benchmark analysis. These data sets are from sparse networks. It is hardly possible to get uniformly consistent and continuous daily observations over this region. Such problems degrade forecast skill. Satellite derived products, for instance TRMM, can provide a good proxy to this. The study seeks to incorporate dynamical products to complement the existing products in the region.

This study therefore addresses prediction challenges on medium range timescale over the Greater Horn of Africa region using the superensemble technique, providing accurate medium scale early warning products for reducing various climate risks that often threaten life, livelihoods and sustainable development.

1.3 Study Objectives

The overall goal of this research was to assess the predictability of precipitation on medium range (up to 10 days) timescale over the Greater Horn of Africa region using the superensemble technique. To achieve this objective, the following specific objectives were undertaken.

i. Assess the space-time distribution of the observed precipitation over the Greater Horn of Africa region.
ii. Evaluate the skill of the ensemble forecasts over the Greater Horn of Africa.

1.4 Justification

Medium range predictions of dry and wet spells are some of the most challenging tasks being addressed in current weather forecasting advancement. Progress on the field is of great benefit to any community since early warning information over such time frame could initiate protective measures and thus, help in minimizing damages associated with weather and climate extremes.

Although seasonal forecasts indicate a below normal, normal or above normal probability events, there is an increased demand from the user community (especially the agricultural sector) for rainfall variability in intra-seasonal timescales. The consistency with which the minimally required rainfall by a plant or crop is more important than the total rainfall received over the season. Crops are likely to do well in evenly distributed 'light' rains than a few isolated'heavy' ones interrupted by prolonged dry periods.

Medium range forecasts of up to 10 days is one of the key priorities at ICPAC and regional NMHSs due to the significant impacts of weather and climate extremes such as floods and drought in the region. Skillful forecasts would be useful for decision making in health, agriculture hydropower, and other socio-economic sectors. Application of a superensemble scheme that takes advantage of the best available model forecasts and generates skillful rainfall prediction would allow more efficient planning and thus improve the quality of life, safety and health.

1.5 Hypothesis of the study

The null hypothesis assumed for this study was that the "Superensemble technique has no significant skill in predicting weather on medium scale over the Greater Horn of Africa region".

1.6 Area of study

The area of study is the Greater Horn of Africa (GHA) region. It lies between longitudes 23.5°E to 52°E and latitudes 21°N to 12°S and has eleven countries namely Kenya, Uganda, Burundi, Rwanda, Tanzania, Somalia, Ethiopia, Djibouti, Eritrea, Sudan and South Sudan. IGAD Climate Prediction and Application Centre (ICPAC) is the designated body in coordinating weather and Climate issues affecting the region in collaboration with the National Meteorological and Hydrological Services (NMHSs).

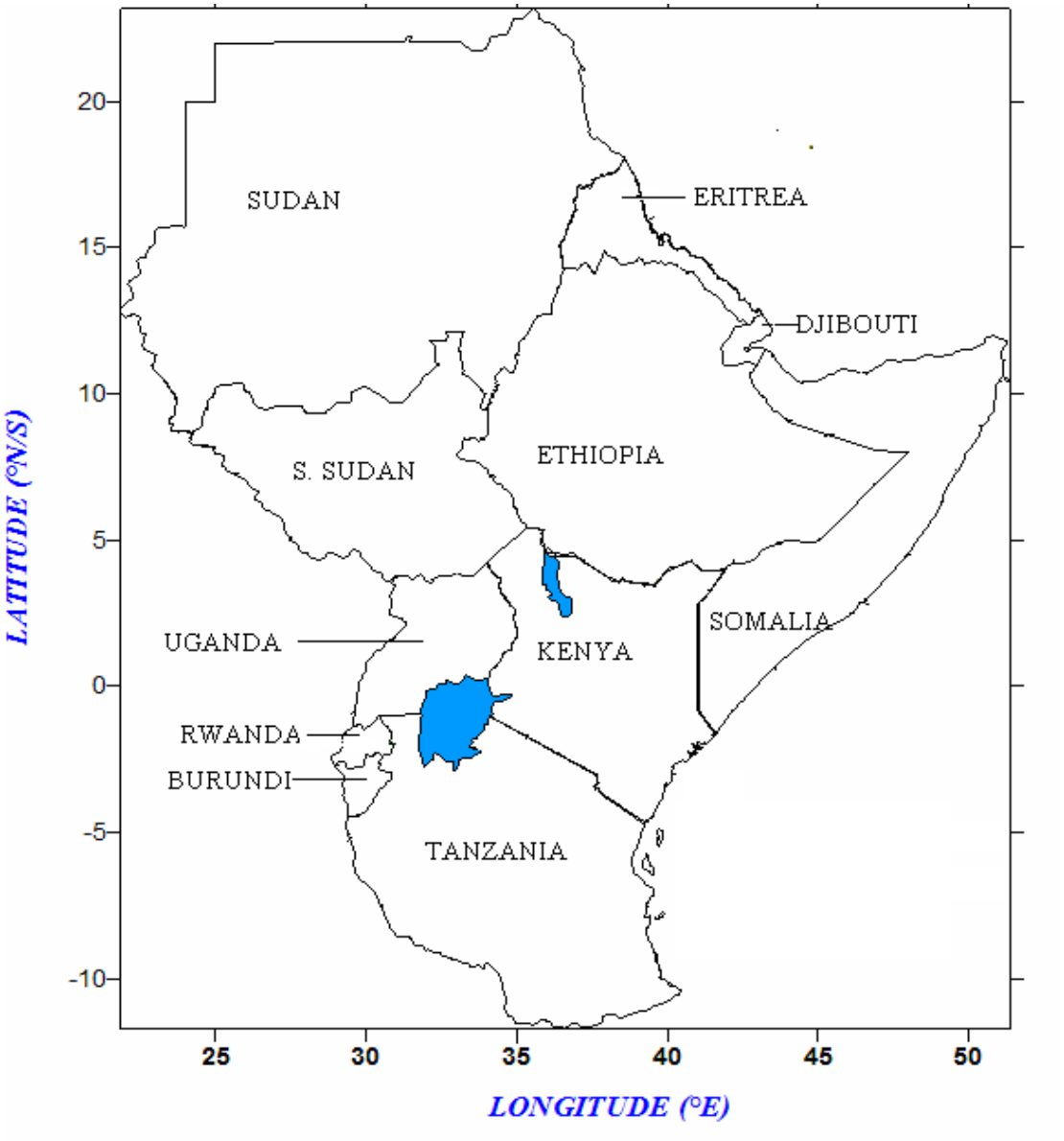

Figure 1: Map of Greater Horn of Africa (Source: ICPAC, 2012)

1.6.1 Physical Features of the Study Domain

The GHA region constitutes of complex and diverse topographical features, a contributing factor to the complexity in weather and climate forecasting. Mt Kenya and Kilimanjaro, for instance, have permanent glaciers at their tops making them potential climate and weather indicators. Others include Mount Elgon (4321 m), Mau escarpment (3098 m), Aberdare Ranges (3999 m), Turkana channel and Ethiopian highlands to the northeast and the East African highlands to the Southwest.

The other unique physical features of the study area include the water masses, for example, Lake Victoria, Lake Tanganyika, Lake Malawi and the Indian Ocean, Eastern and Western Highlands which decline to a plain towards the Indian Ocean. This configuration generates land and sea breezes due to differential solar heating and radiative cooling of the two surfaces. Lake Victoria, for instance has a strong circulation of its own with a semi-permanent trough which migrates from land to lake and lake to land during the night and day respectively.

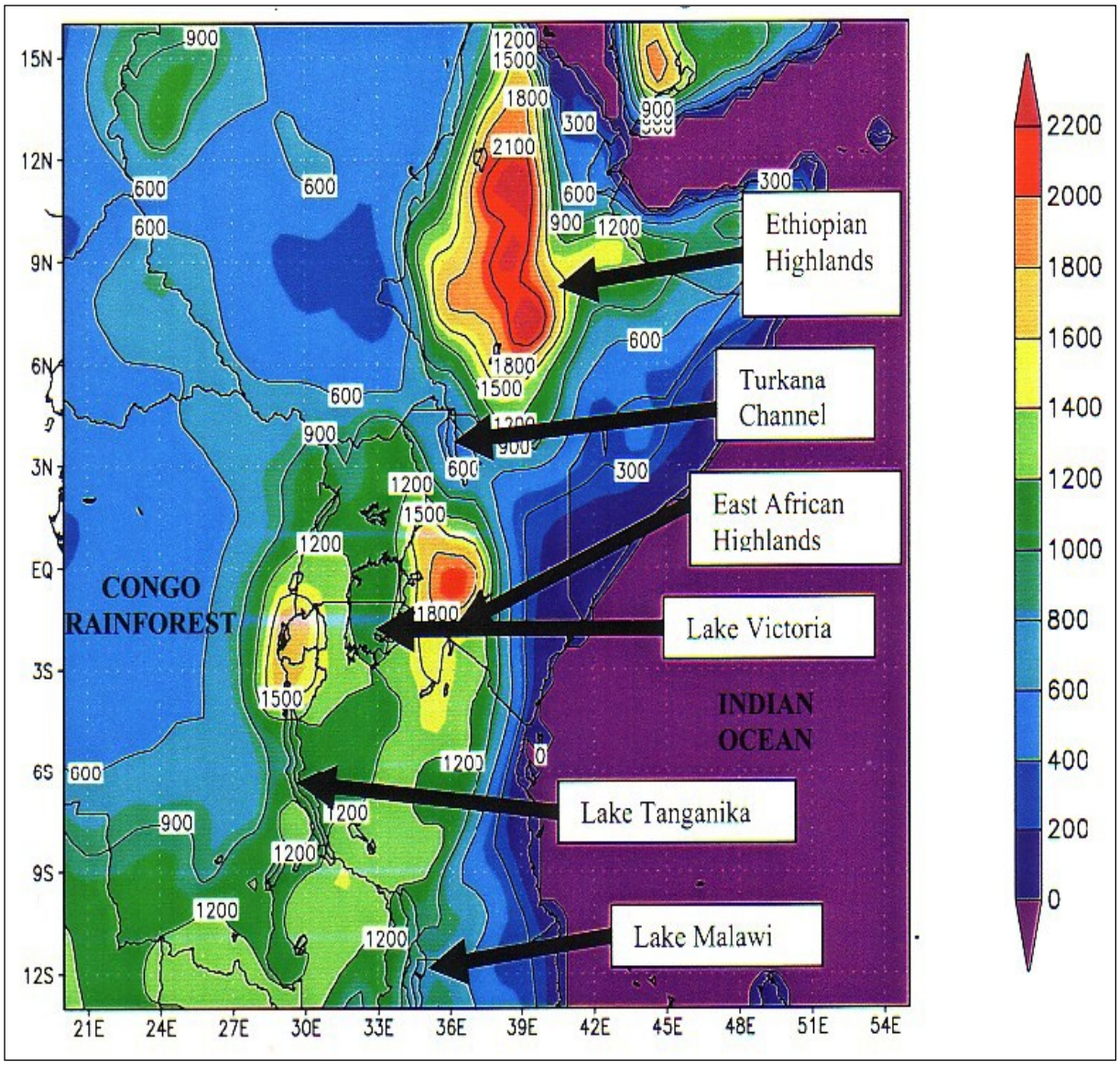

Figure 2: Topographic map depicting physical features of the Greater Horn of Africa. Elevation is in meters (Source: Bowden 2004)

1.6.2 Systems Influencing Rainfall Distribution over the GHA Region

This Section provides a brief description on the systems influencing rainfall distribution over the Greater Horn of Africa region. Systems discussed here are the Inter-Tropical Convergence Zone (ITCZ), Tropical cyclones, El Niño Southern Oscillation (ENSO), Indian Ocean dipole (IOD), Subtropical anticyclones, Quasi-biennial Oscillation (QBO), the interseasonal 30-60 day Madden Julian Oscillation (MJO) and Easterly waves.

1.6.2.1 Inter-Tropical Convergence Zone

Rainfall patterns over the region are controlled by the seasonal migration of the ITCZ. The ITCZ forms a quasi-continuous belt of unsettled, often rainy weather within the tropics, sandwiched between generally fine weather to the north and south of the sub-tropical high pressure belts (Folland *et al.,* 1991).

The ITCZ is associated with the convergence of air streams from the subtropical highs. Where air streams meet, strong upward motion occurs that causes rainfall if the air contains sufficient moisture. It is therefore a region of large scale convergence of the inter-hemispheric tropical monsoonal wind system that generally moves meridionally with the overhead sun. Precipitation is thus controlled majorly by the seasonal migration of the inter-tropical convergence zone (ITCZ). During the OND season, the ITCZ experiences a southward progression and has both the Meridional and zonal arms. The zonal movement of the Meridional component is controlled by the prevailing ocean conditions in the adjacent Atlantic and Indian oceans. For instance, if the Atlantic Ocean sea surface temperatures are colder than that in Indian Ocean, pressure difference between the two oceans leads to zonal variation of the ITCZ. If the alignment is towards the Indian Ocean, strong westerly wind flow is generated causing the advection of Congo air mass towards the region. This air mass is moist, convergent and thermally unstable. This feature is a localized system that enhances precipitation in the region.

1.6.2.2 Tropical Cyclones

Tropical cyclones also play a very vital part in influencing rainfall in the region. They are low pressure systems that form on oceanic areas with sea surface temperatures greater than 26°c. They are cyclonic vortices whose origins are almost invariably in the low

latitudes where the earth's rotation (corriolis force) is sufficient to create a circular motion. Corriolis force increases with increase in latitude. These systems can either cause advection of moisture to or away from the region. In Africa region, they form mostly in the Madagascar region and move towards the land or away.

Tropical cyclones affecting the region form in the southwestern Indian Ocean and Arabian Sea. The tropical cyclone days in the Indian Ocean is linked with higher Quasi-biennial Oscillation (QBO) frequencies, decadal cycles and positive relationship with the sea surface temperatures from September to march (Jury *et al.,* 1999). Effects of tropical cyclones in the region are dependent on its location, and time of the year (Anyamba, 1993). Cyclones that move to the Mozambique Channel can have adverse effects on weather and climate of the region during the March, April, May season. Such an occurrence was observed in 1984 which induced low-level diffluent flow and subsequent suppressed rainfall in the region (Anyamba, 1993).

1.6.2.3 El Niño Southern Oscillation

Another important feature is the El Niño Southern Oscillation (ENSO) phenomenon and associated Teleconnections. These are the fluctuations of sea surface temperatures at the tropical Central and Eastern pacific region (El Niño and La Niña), coupled with the air surface pressure in the tropical pacific (Southern Oscillation). Most regions in GHA receive enhanced rainfall and associated floods during an El Niño year and depressed rains (droughts) during the La Niña phase.

ENSO has significant influence on rainfall over the GHA region (Indeje, 2000; Schreck and Semazzi 2004). It is also linked with the Indian Ocean variability through the modulation of walker circulation. Walker circulation is a zonal circulation of the atmosphere above the Pacific Ocean. It involves the rising of air currents (normally in the west) and sinking of air in the cold oceans (normally in the east). Once in a while ENSO perturbs the Walker circulation and triggers a major change in deep convection and tropical rainfall patterns, disrupting atmospheric circulations and climate across the globe..

An El Niño/ la Nina event is declared based on Oceanic Nino Index (ONI). ONI is a 3 month running average of SST anomalies in the Niño 3.4 region (5^{o}N-5^{o}S, 120^{o}-170^{o}W).

An ONI value greater than +0.5 is an indication of an El Niño event whereas a value less than -0.5 is an indication of a la Nina.

1.6.2.4 Indian Ocean Dipole

Another sea surface temperature related phenomenon with marked influence on the weather and climate of the region is the Indian Ocean dipole (IOD). IOD is a major rainfall indicator within the region. IOD is basically the sea surface temperature gradient between the Western Equatorial Indian Ocean and South Eastern Equatorial Indian Ocean. Dipole Mode Index (DMI) is used to measure the strength of the dipole and it varies between -1°c and 1.5°c with a standard deviation of 0.3. Rainfall in the region has been shown to be above average during the September to December season, when the DMI is greater than one standard deviation above the mean. A positive dipole is associated with enhanced rainfall activities whereas a negative one leads to depressed activities.

1.6.2.5 Subtropical anticyclones

These are regions of high pressure belts in the northern and southern hemisphere, which form the sources of trade winds. They act as pumps of moisture into the low pressure areas. The subtropical anticyclones that have influence on the weather and climate of the region include the Mascarine, St. Helena, Azores, and Arabian high.

The Mascarine and St. Helena high pressure ridge is a major pump of moisture into the region. St. Helena high pressure pumps moisture into the region from the Congo basin which is an important source of moisture to Uganda, Rwanda, Burundi and western parts of Kenya. These areas receive significant rainfall during the period June-August when the high pressure systems in the southern hemisphere are fully developed.

Subtropical anticyclones have a marked influence on the movement and location of the ITCZ. During the Northern Hemisphere summer, the Azores and Arabian highs weaken whereas the St. Helena and Mascarine highs strengthen pushing the ITCZ belt northwards. St. Helena and Mascarine highs weaken during Southern Hemisphere with strengthening of the Northern hemisphere highs leading to a southward shift of the ITCZ.

1.6.2.6 Easterly waves

These are westward propagating wavelike perturbations in the easterly current. They are seen equator-ward of the subtropical high pressure belts near the ITCZ. Their conditions at a specific location depend on location of origin, decay or growth. Easterly waves forming in the Pacific Ocean have been observed to cross the Indian Subcontinent into the Arabian Sea and weaken towards the western Arabian Sea (Asnani, 1993).

Other factors which influence precipitation within the region are tropical storms, jet streams, continental low level troughs, extra-tropical weather systems (Ogallo, 1989), teleconnections with global scale climatic anomalies like those associated with SST, interactions between mesoscale flows and large scale monsoonal flows (Mukabana and Pielke, 1996), the Quasi-biennial Oscillation in the equatorial lower stratospheric zonal wind (QBO), the interseasonal 30-60 day Madden Julian Oscillation (MJO) (Anyamba, 1992), solar and lunar forcing (Ogallo, 1988; Indeje and Semazzi, 2000), and local factors such as topography and water bodies.

CHAPTER TWO

2.0 Literature review

Rainfall prediction in the tropical region remains one of the most challenging problems in weather forecasting. Numerical models often do not reproduce the correct rain rate despite using analyses which have been produced by sophisticated data assimilation schemes.

Many studies on the short to medium range scales have been undertaken by various researchers in the Greater Horn of Africa region with the sole aim of improving the prediction skill. Mukabana and Pielke (1996) noted that the short range rainfall forecasts over the Greater Horn of Africa are based on surface and upper air analysis of synoptic systems and mesoscale circulations. However, this method is only able to give subjective and qualitative forecast. In order to perform objective and quantitative predictions, numerical weather prediction models should be utilized.

Mutemi *et al*., (2007) analyzed the forecasts of rainfall events over some regions of Africa. Results showed that the FSUSE RMSE, ETS, and the bias on the daily forecasts of rainfall were invariably superior to the best member model. Anyamba (1992) studied on the temporal variability of the 40-50 day oscillation in tropical convection. Results showed that apart from the well-known 40–50-day peak, there are other significant spectral peaks near 20–30 and 17 days. In much of the tropics, excluding the equatorial Indian and western Pacific Oceans, these higher frequency peaks appear to be distinct from the 40–50 day spectral peak.

Webster *et al.,* (1998) found out that the dynamical predictions suffer from a consistently large ensemble spread, which is compatible with the theory that chaotic weather systems in the southern Hemisphere may trigger breaks in the Asian monsoon, providing short term predictability, but limiting seasonal predictability.

Nicholson, (2014) examined the predictability of seasonal rainfall over the Greater Horn of Africa. He examined the predictability of each of the three rainy seasons affecting the Horn of Africa is using multiple linear regression and cross validation. He noted that atmospheric variables generally provide higher forecast skill than surface variables, such

as sea surface temperatures and sea level pressure, and that ENSO and the Indian Ocean dipole provide less forecast skill than atmospheric variables associated with them.

Lee (2014) examined the usefulness of proxy quantitative precipitation estimates (QPEs) from the Self-Calibrating Multivariate Precipitation Retrieval (SCaMPR) algorithm for modeling hydrological processes. He made use of two sets of SCaMPR QPEs, one with Tropical Rainfall Measurement Mission (TRMM) version 6 data integrated and the other without as key forcing to the lumped National Weather Service (NWS) hydrological tool to study and generate flow simulations for 10 catchments areas in Texas over the period 2000–07. The year 2000 data was used for the model spin up, 2001–04 for calibration, and 2005–07 for validation and later validated the results using observed stream flow alongside similar simulations obtained using interpolated gauge QPEs with varying gauge network densities, and still others using the operational radar–gauge multi-sensor product (MAPX). He noted that calibrating the model using individual QPEs rather than the MAPX (the most accurate QPE), yielded overall improvements to the simulation accuracy but did not change the relative performance of the QPEs.

Omeny *et al.,* (2008) studied the effects of MJO on rainfall Variability over the East African region. He found out high association between rainfall and MJO indices and relatively high skill of predicting intra-seasonal rainfall over the west than the east.

A comparative verification of the quantitative precipitation forecasts for UKMO, NCEP and MM5 NWP models have been carried out (Gitutu, 2006) over Kenya. He examined the level of skill of daily precipitation forecasts of numerical weather prediction (NWP) models where in all the models the RMSE was found to be largest during the rainy season of MAM and relatively low for the drier months. The RMSE was particularly high on occasions of heavy precipitation where all the models failed to simulate for the case of Lamu and Marsabit stations in July. There were no other significant differences between the models that could be discerned other than slightly large errors produced by the NCEP model. It was therefore noted that no model was better than the other in terms of accuracy and skills.

Krishnamurti *et al.,* (1999) showed that models over the tropics still show low predictability of rainfall. In contrast to this scenario, middle and higher latitudes depicts

relatively good accuracy in simulating the observed weather and this is attributed to the multilevel numerical modeling.

Kibara (2011) looked into the predictability of weather on extended NWP time scales over Kenya using the NCEP GFS model. He found out that OND season is influenced by large scale systems. He also showed that the model was able to capture the wet events. However, it couldn't capture well the dry events as there were incidents of false alarm and under-forecasting.

Various studies have discussed extensively the multi-model short range predictions. Doblas-Reyes *et al.,* (2000) combined seasonal forecasts from four different Atmospheric General Circulation Models (AGCMs) and found minimal skill improvement. Studies on the seasonal scale have also been undertaken by various researchers. Okoola *et al.,* (2008) studied on the Wet periods along the East African Coast and the extreme wet spell of October 1997. The study showed a high spatial consistency in the precipitation over the EAC. The circulation features that were common during most of the wet events were westward-moving disturbances in the low-level Equatorial wind field, enhanced convergence between the Northern Hemisphere (NH) and Southern Hemisphere (SH) trade winds and weakening or reversal of the zonal (Walker type) circulation over the Indian Ocean.

Anyah and Semazzi (2007) looked into the variability of East African rainfall based on multi-year RegCM3 model simulations. Their findings showed that spatial correlation between the global teleconnections and the simulated seasonal precipitation and some of (DMI and Nino3.4 indices) showed that the regional model conserves some of the observed regional features where rainfall-ENSO/DMI associations are strong.

Ininda et al., (2008) researched on Seasonal Rainfall Forecasting through Model Output Statistics (MOS) Downscaling of ECHAM forecasts over Tanzania. The results indicated that the model was capable of simulating the observed climatological circulation and the annual rainfall pattern over Tanzania. The skill of simulation was highest during the October to December (OND) rainfall season where the model explained as high as 74% of the variance at some locations while during March to May (MAM) the variance explained over most locations was less than 40%. This result was consistent with the

previous studies that have shown high (low) correlation between the OND (MAM) rainfall and the SST. Moreover, the El Nino Southern Oscillation (ENSO) signals are observed to be stronger during the OND season. The results from the study showed that the use MOS for down scaling improves the simulation skill.

Mutemi (2003) used ECHAM4.5 to study the variability of East African climate. The model reproduced the climatological mean pattern such as the bimodal seasonality of rainfall associated with the north–south migration of the ITCZ and monsoonal flow. The study however did not get the correct amplitudes of the inter-annual variability linked to extreme El Nino episodes such as the 1982 and 1997. The skill of ECHAM4.5 over East African sub region has been addressed by IRI/ICPAC collaboration (2002). The results indicated that ECHAM4.5 was the best model especially between July-December months. The skill of the model was found to be higher during ENSO when large SST values are found over many parts of the Equatorial tropics.

Ogallo *et al.,* (1979) performed a time series analysis for 69 stations in Africa. Trend analysis revealed that most of the annual series indicate some forms of oscillations rather than any particular trend. He showed that use of binomial coefficients to smooth the series indicated positive or negative trends in recent years in 20 series, but only four of these were statistically significant judging by the Spearman rank correlation test.

Omondi (2010) studied the Linkages between global sea surface temperatures and decadal rainfall variability over Eastern Africa region. The study revealed that forcing of decadal precipitation over the region is linked with El Niño mode that is prominent over the Pacific Ocean, while Indian Ocean dipole is the most important mode over the Indian Ocean. An inter-hemispheric dipole mode that is common during ENSO was a prominent feature in the Atlantic Ocean forcing regional decadal rainfall.

In an extensive evaluation of FSUSE technique for numerical weather prediction over a global domain within 55 S-55 N, Ross and Krishnamurti (2005) showed that the scheme gives forecasts results that are superior to the member models and the ensemble mean in forecasts of mass field , motion field, and precipitation. For example, the authors found that Superensemble improved the worst model daily forecasts by 37% for day 1, 44% for day two, and 43% for day 3. On a season to season comparison, the transition seasons of

fall and spring were forecasted with much better skill than the extreme seasons of summer and winter. The Southern hemisphere models depicted larger and consistent systematic errors which the multi-model Superensemble is able to capitalize on in the training period to provide good results.

The inter-annual variability of precipitation is extremely consistent throughout most of the East Africa despite quite diverse climatic mean conditions. The biggest portion of this variability is accounted for by the short rains season of OND (Mutai *et al.,* 1998).

Sakwa (2006) examined the skill of the High Resolution Regional Model in the simulation of airflow and rainfall over East Africa. He found out that the model simulated well though with some few cases of under estimation and overestimation. The experiment revealed that finer model resolution produced statistically significant improvements with the study recommending the use of ensemble schemes in Kenya.

It is important to note that Global Circulation Models differ in many aspects including their resolution, physics and dynamics, representation of orography, initialization and data assimilation. Operationally, dynamical models do not perform equally well in different regions due to lack of data to correctly define initial conditions and the complex terrain. Moreover, the skillful performance of these models should be treated cautiously, considering their resolution. NWP quality evaluation determines the confidence related to a particular forecast over a specific region. However, the evaluation can also be thought of as a preliminary validation of simulated climate drift that can be expected from the model being tested. This idea is further illustrated by (Kamga *et al.,* 2000) who analyzed the systematic errors of the ECMWF operational model (120h forecast). From this point of view, verification of model products can serve local forecast applications and a wider community that conducts research on a variety of timescales using global model forecasts and analyses.

Kirtman *et al*., (2003) showed that a major stumbling block to the improvement of the skill of forecast is model error, as seen in the long-term simulations. He noted that all coupled models have serious systematic errors in terms of the mean, the annual cycle or the statistics of inter-annual variability and, in some cases, all three of these characteristics.

Operationally, model errors are still a shortcoming in forecasting (Latif et al, 2001). Model agreement with observation of current weather and climate is the only way to assign model confidence. A number of techniques have been proposed to improve the analysis of the moisture and divergence fields (Donner *et al.,* 1999; Heckley *et al.,* 1990; Puri and Miller, 1990; Puri and Davidson, 1992; Aonashi, 1993; Kasahara *et al.,* 1994).

One of the techniques proposed to improve the analysis of moisture and divergence fields is the physical initialization (PI) procedure. Krishnamurti *et al.,* (1984; 1988; 1991) and Treadon (1996) have shown that there is a dramatic increase in the now casting skill of precipitation, with a subsequent improvement in the one-day forecast. The PI technique assimilates observed precipitation (often satellite derived) using a reverse cumulus algorithm, along with reverse algorithms for the physical process.

With all these model shortcomings however, many authors have been able to achieve appreciable progress. Many scientific efforts have been made to provide the best of precipitation and temperature forecasts (Rajeevan *et al*., 2006). That progress largely came from a statistical multiple regression approach that included a number of predictands.

The ensemble prediction schemes, single or multi-model, is a relatively recent contribution to the general area of weather and climate forecasting. Most deterministic and probabilistic ensemble forecast is produced with a single dynamical model, although sometimes a set of multi-models is used. The skill of a single and multi-model ensemble has been reported by many studies (Doblas-Reyes *et al.*, 2000; Graham *et al.* 2000; Palmer *et al*., 2000).

Such ensemble techniques are nowadays routinely used at operational weather forecasting centers (Molteni *et al*., 1996; Buizza, 1998; Toth and Kalnay, 1997). They are also applied in seasonal timescale climate studies (Brankovic and Palmer, 1997; Zwiers, 1996; Doblas-Reyes 2000; Peng *et al*., 2002).

Palmer *et al.,* (2004) noted that ensemble modeling is now routinely applied on essentially all time scales, ranging from the scale of weather forecasts to the scale of climate-change scenarios. Its success has been demonstrated in many studies where simple ensemble models can be constructed by pooling together the available single

model predictions with equal weight. Straus and Shukla (2000) demonstrated that different models have its own variability generated by internal dynamics. As a result, the performance of a multi-model ensemble is generally more reliable than that of a single model.

Goerss (2000) examined the usefulness of putting together three dynamical models into an equally weighted ensemble mean. He used GFDL, NOGAPS, and United Kingdom Meteorological Office. The resulting ensemble mean showed greater skill than the majority of single models.

Kirtman *et al*., (1997) found that a combination of physical ocean models, AGCMs and statistical models is useful in predicting seasonal rainfall because different models addresses different problems. However, given that models may differ in their quality and skill, it has been suggested to further optimize the effect by weighting the participating models according to their prior performance in its simplest form.

Several approaches have attempted to combine model ensemble forecast to a single reliable forecast that carries higher skills when compared to the individual member models. These include the simple ensemble mean (Peng *et al.,* 2002; Doblas-Reyes *et al.,* 2000; Palmer *et al.,* 2004), regression improved ensemble mean (Kharin and Zwiers, 2002), bias removed ensemble mean (Kharin and Zwiers, 2002), and the multi-model Superensemble (Krishnamurti *et al.,* 1999).

Veenhuis (2013) researched on the spread calibration of Ensemble Model Output Statistics (MOS) Forecasts. He used a post-processing ensemble technique called kernel density model output statistics (EKDMOS). Forecasts from this technique had an improved calibrated spread–error relationship, and showed increased day-to-day spread variability and were more reliable.

Calvetti and Filho (2014) carried out a research on Ensemble Hydrometeorological Forecasts using Weather Research and Forecasting (WRF) hourly Quantitative precipitation forecast (QPF) for the Iguaçu river watershed (IRW) in southern Brazil. He found out that the ensembles yielded up to 20% better skill than single WRF forecasts for the events analyzed.

Following intensive studies (Krishnamurti *et al.,* 1999; 2000b; 2005; Williford *et al*., 2003), at FSU, the multi-model forecast data set constitutes a valuable basis upon which the super ensemble has evolved.

Krishnamurti *et al*., (2000a) and Chaves *et al.,* (2005) showed that Superensemble is a powerful post-processing tool that makes use of forecasts from global producing centers. The technique has been proven to be successful in producing a deterministic forecast superior not only to any of the individual models going into it, but also to the multi-model ensemble forecast. Research so far has been done on the Superensemble as a deterministic forecast, and it has been shown that using the Superensemble method leads to a significant reduction in RMSE.

The superensemble methodology (Krishnamurti *et al.,* 1999) issues a consensus forecast from a set of dynamical model forecasts by applying a collective bias correction in a manner unlike classical bias corrections. The latter weight every model equally both in bias calculation and forecast construction. In contrast, the Superensemble technique considers the past performance of each model in assigning its relative forecast weight. This is carried out for each of the models, variables and at every grid location.

The technique has been shown to yield superior forecasts when applied to weather and climate prediction (Krishnamurti *et al*., 2000a;2000b; 2001; 2002; 2003; Chakraborty *et al.,* 2006)

Its algorithm entails the division of a time line into two parts, a training phase and a forecast phase. In this technique, the different model forecasts are statistically combined during the training phase using multiple linear regression with the skill of each ensemble member implicitly factored into the Superensemble forecast. The least square minimization method leads to calculation of statistical weights.

Weights calculated vary geographically, thus taking into account the regional variation and biases of each model. The weights therefore make the Superensemble an exceptional tool compared to other ensemble schemes (Stefanova and Krishnamurti, 2002; Chakraborty and Krishnamurti, 2006).

Mutemi *et al.*, (2006) noted that as the number of training Days increases successively from 60, 90, 120 and 150, the RMSE continues to decrease. He found out that roughly 150 days of training are minimally needed for improved forecasts.

The forecast resulting from the projection of these weights into a forecast phase has small errors and higher skill than most conventional models and conventional ensemble techniques. The ensemble mean assigns a weight of 1/N to each of the N member models everywhere regardless of their relative performance. As a result assigning the same weight of 1/N to some poorer models has been noted to degrade the skill of the ensemble mean. It is possible to remove the bias of models individually and to compute an ensemble mean of the bias-removed models. This too has somewhat lower skill compared to the Superensemble, which carries selective weights distribution in space, multi-models, and variables.

The skill of the multi-model superensemble method significantly depends on the error covariance matrix since the weights of each model are computed from a designed covariance matrix. The classical method for the construction of the superensemble utilizes a least square minimization principle within a multiple regression of model output against observed 'analysis' estimates. This entails a matrix inversion that is solved by Gauss Jordan elimination technique. The matrix can be ill-conditioned and singular depending on the interrelationships of the member models of the superensemble. Recently designed (Wilks, 1995) based on is a singular value decomposition (SVD) method for the multi-model superensemble that overcomes this problem and removes the ill conditioning of the covariance matrix entirely (Yun *et al.*, 2003). Tests of this method have shown great skills in weather and seasonal climate forecasts compared to the Gauss Jordan elimination method.

Many enhancement of the superensemble technique have been made in past studies (Krishnamurti *et al*., 2001; 2003; Stefanova and Krishnamurti, 2002; Yun *et al*., 2003) and it has been shown that this technique provides higher skill forecasts compared to all participating member models and the ensemble mean. Krishnamurti *et al.*, (2003) noted that the Superensemble skill during the forecast phase could be degraded if the training was executed with either poorer analysis or poorer forecasts. This indicates that the

forecast will be improved when higher quality training data sets are deployed for the evaluation of the multi-model statistics.

A mix of multi-model based medium range forecasts and a comprehensive downscaling and the construction of Superensemble from model outputs is therefore the approach to be followed in this study. The availability of a comprehensive rainfall data archive from TRMM at a horizontal resolution of 25km and the model output from the Global Circulation Models will make this process possible.

CHAPTER THREE

3.0 DATA AND METHODOLOGY

This chapter is devoted to the discussion of the data and the various methods employed to achieve the main objective.

3.1 Data

The data used in this study included rainfall estimates from Tropical Rainfall Measuring Mission (TRMM) and model outputs from THORPEX (The Observing system Research and Predictability Experiment) Interactive Grand Global Ensemble (TIGGE).TIGGE datasets is an effort by the World Weather Watch Programme to improve on the forecast skill of 1 day to 2 weeks.

3.1.1 Satellite Rainfall Estimates

Although the National Meteorological and Hydrological Centers (NMHCs) all over the world have a network of observing stations, they are not dense enough. Data from such stations are thus not adequate and cannot be used as a representative of a very large area. TRMM, which is a joint venture between National Aeronautics and Space Agency (NASA) and Japan Aerospace Exploration Agency (JAXA), is therefore, a grand idea as they provide high resolution data (25km) spanning the entire tropical belt.

TRMM has been availing accurate observational sets of precipitation over the global tropics since its launch on 27 November 1997. It was designed to monitor tropical and subtropical precipitation and to estimate its associated latent heat using precipitation radar (PR) and the TRMM Microwave Imager (TMI) instruments (Kummerow *et al.,* 2000).

The algorithm used is the TRMM Microwave Imager (TMI) 2A12 rainfall algorithm, (Kummerow *et al*., 1996; 2000) that is supplemented by the National Oceanic and Atmospheric Administration/ National Environmental Satellite, Data, and Information Service Special Sensor Microwave/Imager (NOAA/NESDIS SSM/I) algorithm (Ferraro *et al.,* 1995).

The TRMM satellite has 5 sensors on board, which are precipitation radar (PR), TRMM Microwave Imager (TMI), Visible Infrared Scanner (VIRS), Clouds and the Earths Radiant Energy System (CERES), and Lighting Imaging Sensor (LIS). PR, TMI, and VIRS are sensors for measuring the rain, but the observation principle and the swath width of each sensor are different from each other. PR measures three dimensional distribution of rainfall by means of receiving retuned signals from the rain after it transmits a microwave.

3.1.2 Model Output (Hind casts)

Model outputs from THORPEX Interactive Grand Global Ensemble (TIGGE) were used in this study. Most operational Numerical Weather Prediction (NWP) centers run models that span the global domain. These centers have jointly agreed to provide their outputs to TIGGE. TIGGE is a noble idea that envisages a world free of weather related catastrophes by routinely providing real time daily weather forecasts from ten global centers for research purposes. These centers are the European Centre for Medium Range Weather Forecasts (ECMWF), the National Centre for Environmental Prediction (NCEP), the Center for Weather Forecast and Climatic Studies (CPTEC), the China Meteorological Agency (CMA), the Canadian Meteorological Centre (CMC), the United Kingdom Meteorological Office (UKMO), the Australian Bureau of Meteorology (BOM), the France Meteorological Agency (MeteoFrance), the Korea Meteorological Agency (KMA) and the Japan Meteorological Agency (JMA). A brief description of the TIGGE models is provided in Table 1.

In this study, the FSUSE utilizes outputs from four centers namely ECMWF, NCEP, CPTEC and UKMO to make consensus forecasts of up to 10 day lead time by utilizing the Superensemble technique. The four center models were chosen based on their consistency in terms of runs and data availability and forecast data validity time (12.00 GMT). Validity time was taken to be 12.00 GMT so as to coincide with the TRMM data.

TIGGE is therefore a key component of World Weather Watch Programme attempt to improve on the forecast skill for the medium range scales of 1 day to 2 weeks and also bridge the gap that exists between the academic and operational worlds.

Table 1: Descriptions of NWP models from the TIGGE archive

Data provider	**BoM**	**CMA**	**CMC**	**CPTEC**	**ECMWF**	**JMA**	**KMA**	**METEOFRA**	**NCEP**	**METOFF**
Horizontal resolution	1.5° x1.5°	0.56°x 0.56°	1.00° x1.00°	1.00° x1.00°	TL399	1.25° x1.25°	O.56° X0.38°	1.50° x1.50°	1.00° x1.00°	0.83°X 0.56°
model levels	19	31	40	28	62	60	70	65	28	85
Runs per day (UTC)	*2 (00, 12)*	*2 (00, 12)*	*2 (00, 12)*	*2 (00, 12)*	*2 (00, 12)*	1(12)	4(00,06,12,18)	2(06, 18)	4(00,06,12,18)	2(00,12)
Coupled to an ocean model?	NO	NO	NO	NO	NO	NO	NO	NO	NO	NO
Top of model	*~10 hPa*	*~10 hPa*	*~2 hPa*	*~0.1hPa*	*~5hPa*	~0.1 hPa	~80 Km	~50 Km	~2.73 hPa	~85 Km

3.2 Methodology

This Section presents the various methods employed in this study to achieve the set objectives. Subsection 3.3.1 addresses the first objective which involves the assessment of the Spatial and temporal Distribution of Observed rainfall. 3.3.2 And 3.3.3 involves the assessment of model skill and measures of accuracy and the superensemble methodology respectively.

3.2.1 Assessment of the Spatial and temporal Distribution of Observed rainfall

This subsection was examined by use of simple spatial and temporal analysis that included time series plots and spatial maps. Spatial maps and time series plots were obtained by use of Grid Analysis and Display System (GrADS) software.

3.2.2 Assessment of model skill and measures of accuracy

This section presents various statistical measures of accuracy and goodness used to assess skill of SE performance in this study. These include Root Mean Square Error (RMSE), Spatial Correlation (SC), Bias and Equitable Threat Scores (ETS).

3.2.2.1 Root mean square error

Root mean square error is a measure for computing the differences between values predicted by a model and the actual observations and is represented by the Equation 1.

$$RMSE = \sqrt{\frac{1}{N}\sum_{i=1}^{N}(F_i - O_i)^2} \quad \text{.....1}$$

In Equation 1, N is the total number of the observations or the forecasts, $\boldsymbol{F_i}$ and $\boldsymbol{O_i}$ are the predicted and the observed values at time i.

3.2.2.2 Spatial Correlation analysis

Correlation analysis provides the degree of linear association between a pair of variables. The simple correlation coefficient (r) between a model output variable **(f_i)** and the corresponding observation **(o_i)** is given by Equation 2.

$$r = \frac{\frac{1}{N}\sum_{i=1}^{N}(f_i - \bar{f})(o_i - \bar{o})}{\left[\frac{1}{N}\sum_{i=1}^{N}(f_i - \bar{f})^2.(o_i - \bar{o})^2\right]^{1/2}} \quad \ldots\ldots 2$$

In Equation 2, $\bar{o}$ and $\bar{f}$ are sample means of observed data and model outputs, respectively, and N is the total number of cases used in the analysis. The r value indicates the correlation of the forecasts to the observation; a high (low) r value indicates higher (lower) correlation between the two.

Correlation alone is not sufficient to delineate linkages between multiple dependent/ independent variables. The statistical significance of r may be tested using the standard student t-test. Test significance level to be considered is 95% confidence. If found that computed value of t is greater than tabulated value, then correlation coefficient is significant. This will be done using Equation 3.

$$t_{n-2} = r\sqrt{\frac{n-2}{1-r^2}} \quad \ldots\ldots 3$$

Spatial correlation gives the areal average performance of a forecast. For this study, a grid by grid mapping between the forecast and observed rainfall values were done to establish the overall performance of the models.

3.2.2.3 Equitable Threat Scores and Bias Scores

The Equitable Threat Score (Schaefer, 1990) measures the skill in predicting the area of precipitation amounts over any given threshold with respect to a random (no skill) control forecast and is defined by Equation 4.

$$ETS = \frac{(H - CH)}{(F + O - H - CH)} \quad \ldots\ldots 4$$

In Equation 8, F is the number of grid boxes that forecast more than the threshold, O is the number of grid points that observe more than the threshold, H is the number of grid points that correctly forecast more than the threshold and CH is the expected number of hits in a random forecast of F points for O observed points. CH is expressed as shown in Equation 5.

$$CH = \frac{(F*O)}{T} \quad \text{.....5}$$

In Equation 5, T is the total number of grid boxes inside the verification domain. The ETS seems to be a good estimate for overall forecast skill. The higher the ETS value, the better the forecast skill for that particular threshold. It can vary from a small negative number to 1.0, where 1.0 represents a perfect score. The ETS is basically the ratio of the correct forecast area to the total area of the forecast and observed precipitation. The model gets penalized for forecasting rain in the wrong place as well as for not forecasting rain in the right place. Therefore the model with the highest score is the best model.

Bias score is the ratio of the forecast area (points) to observed area (points) of precipitation amounts over any given thresholds (Anthes, 1983). It is defined by Equation 6.

$$BIAS = \frac{F}{O} \quad \text{.....6}$$

Bias score is a very simple equation. It does not comment at all on the skill of a model forecast in terms of placement of precipitation, but does give an indication if a model is consistently over-forecasting or under-forecasting rainfall areas. A model that remains near the 1.0 line is the best. If the model verifies over 1.0, it is over-forecasting and if below 1.0 then it is under forecasting.

3.2.3 Superensemble Methodology

The super ensemble approach is a recent contribution to the general area of weather and climate forecasting. This has been discussed in a series of publications (Krishnamurti *et al.,* 1999; 2000a; 2000b; 2001).

The technique entails the partitioning of a timeline into two parts. One part is the control (training) phase, where forecasts by a set of member models, are compared to the observed field. This is done in order to develop statistics i.e. weights a_i (Equation 7) on the least squares fit of the forecasts to the observations. The second part is the forecast phase where weight estimates from the training phase are used to create the superensemble.

The performance of the individual models is thus obtained in the training phase using multiple linear regressions against observed (analysis) fields. The outcome of this regression is the weights assigned to the individual models in the ensemble, which are then passed on to the forecast phase to construct the Superensemble forecasts. The temporal model anomalies of the variables are regressed against the observed anomalies when formulating the Superensemble forecasts, and the weights are multiplied to the corresponding model anomalies. The constructed superensemble forecast is as shown in Equation 7.

$$S = \sum_{i=1}^{N} a_i \left(F_i - \bar{F}_i\right) + \bar{O} \quad \ldots\ldots 7$$

In Equation 7, $\bar{O}$ is the observed climatology over the training period; a_i is the weight for the i^{th} member in the ensemble; and F_i and $\bar{F}_i$ are the i^{th} models forecasts and the forecast mean (over the training period) respectively. N is the number of member models. The weights a_i are obtained by minimizing the error term E, where E is expressed as shown in Equation 8.

$$E = \sum_{t=1}^{N_{train}} \left(S_t' - O_t'\right)^2 \quad \ldots\ldots 8$$

In Equation 8, N_{train} is the number of time samples in the training phase, and S_t' and O_t' are the respective superensemble and observed field anomalies at training time t. This exercise is done at all model grid points. A fit performed for all model variables at all model grid points at all vertical levels typically yields close to 10^7 regression weights. These spread of weights are fractional, positive or negative. This large number arises from the number of transform grid points, number of vertical levels, number of basic variables and the number of models. Over many such locations, diverse performance characteristics of the member models that arises from differences in horizontal and vertical discretization, treatment of physics, handling of inhomogeneity of land surface, orography, water bodies, surface physics and boundary conditions have been noted.

3.2.3.1 Downscaling methodology

The daily mean datasets from the multi-models was interpolated to 0.25^{o}x0.25^{o} resolution for the period 1997-2013 to conform to the TRMM resolution. This was done by use of bilinear interpolation. The procedure involves calculation of regression coefficients which can be done using Equation 9.

$$R_{obs} = aR_{mdl} + b + e \quad \text{.....9}$$

In Equation 9, R_{obs}, $\mathrm{R_{mdl}}$, a, b and e are the observed rainfall, interpolated model forecasts, regression coefficient and the error term respectively. The basic principle here is to minimize the absolute value of the error term ($\left|\mathrm{e}\right|$). Downscaled model rainfall is then obtained using these coefficients.

$$R_{dscl} = aR_{mdl} + b \quad \text{.....10}$$

From Equation 10, R_{dscl}, (a) and (b) are the downscaled rainfall forecast of the model, slope and the intercept of the least square fitting. The regression coefficients (a) and (b) are computed using Equation 3 at each grid point and separately for each day. They carry information that varies temporally and spatially and are to be used to predict the regional precipitation over GHA. The schematic procedure for downscaling and Superensemble forecasting is as shown in Figure 3.

(a)

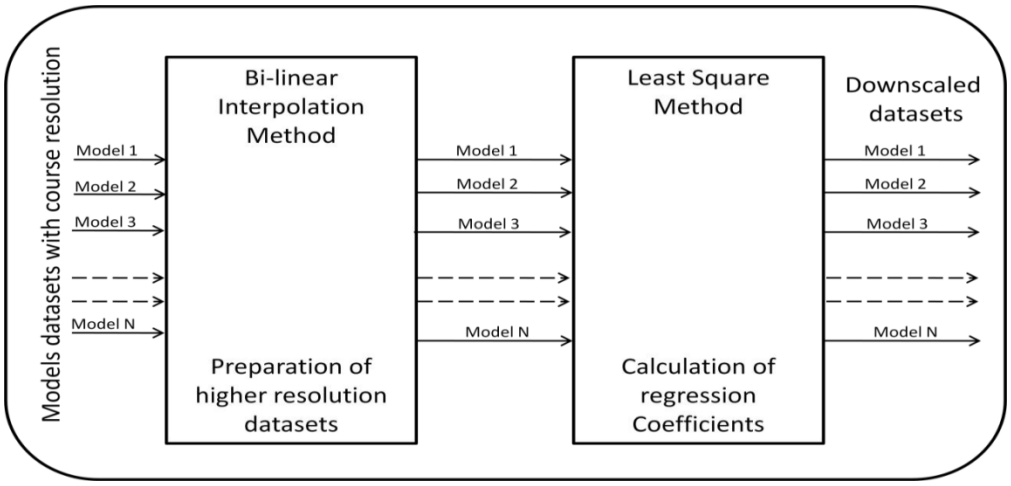

(b)

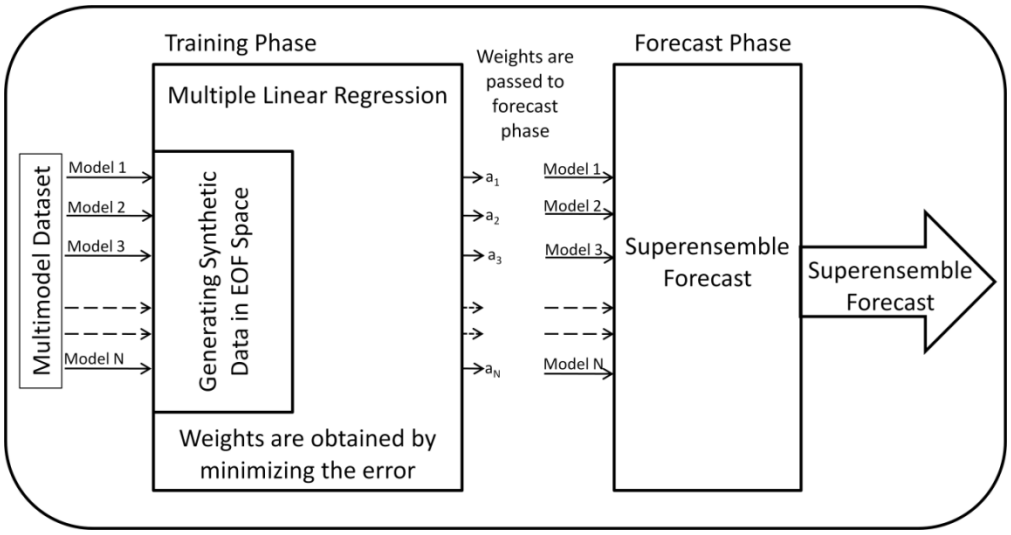

Figure 3: Schematic diagram showing the steps involved in: (a) Downscaling methodology, and (b) Superensemble forecasts. The model's forecasts are statistically evaluated for their errors during the training phase and the resulting statistical weights are used to construct the multi-model super ensemble (adapted from Krishnamurti, 2010)

CHAPTER FOUR

4.0 RESULTS AND DISCUSSIONS

This chapter presents the results obtained in this study. Spatial and temporal distribution of the observed rainfall and forecast skill scores of TIGGE multi-models and the final Superensemble ten day rainfall forecasts are presented.

4.1 Spatial and temporal distribution of the observed precipitation over the Greater Horn of Africa Region

Rainfall estimates from the Tropical Rainfall Monitoring Mission were used. The assessment was done by use of spatial and temporal analysis that included the use of spatial maps and time series plots. This was done in a series of intervals spanning the ten day and monthly average distribution for the period 2008 to 2010.

Figure 4 shows the distribution of observed (TRMM) 10 day mean rainfall (in mm/day) over the GHA region during the months of October to December 2008. The figure shows that in the first dekad of October, much of Western Kenya, Uganda, South Sudan, Southern Ethiopia and Southern Somalia received rainfall amounts of between 1.0 mm/day to 10 mm/day with some small patches near the Lake Victoria region receiving up to 20 mm/day. These amounts can be seen in Figure 4 (a). There were no much changes in the second dekad. During the third dekad of October and first dekad of November, a north easterly shift of rainfall activities were noted with rainfall amounts between 30 mm/day to 50 mm/day recorded in Central Eritrea (Figure 4 c, and d). During the last two dekads of November (Figure 4 e and f) and all the December dekads (Figure 4 g, h and i) for the period 2008, much of the northern sectors of the GHA remained dry. Much of Sudan, South Sudan, Eritrea, Djibouti and Somalia; most parts of Ethiopia and Northern Kenya received less than 1.0 mm of rainfall. Over the same period, the south western sector of the region including Western Kenya, Most parts of Tanzania, Uganda, Rwanda and Burundi received rainfall amounts between 2.0 mm to 15.0 mm (Figure 4 e and f).

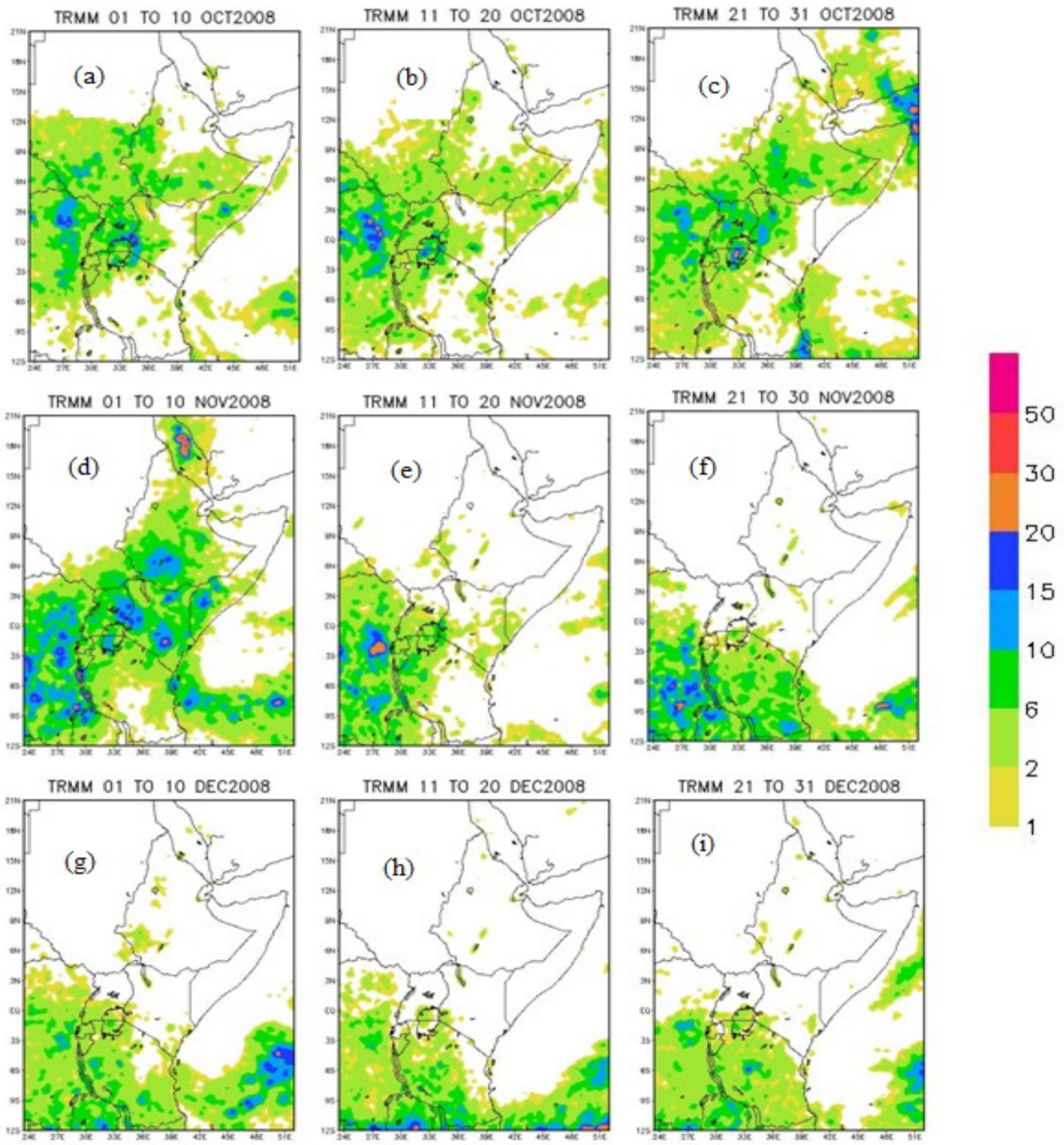

Figure 4: Spatial distribution of observed (TRMM) 10 day mean rainfall (mm/day) over the GHA region during the months of October to December 2008

Figure 5 shows the distribution of observed (TRMM) 10 day mean rainfall (in mm/day) over the GHA region during the months of October to December 2009. Figure (a), (b) and (c) shows rainfall distribution for the month of October. It is evident that the rains are concentrated in the equatorial sector during the months of October with a slight southward shift in the November month. By December, the rains are fully concentrated in the south (Figure g, h, and i). Coastal Kenya and South Somalia received rainfall amounts of between 30 mm/day to 50 mm/day (Figure 5 c).

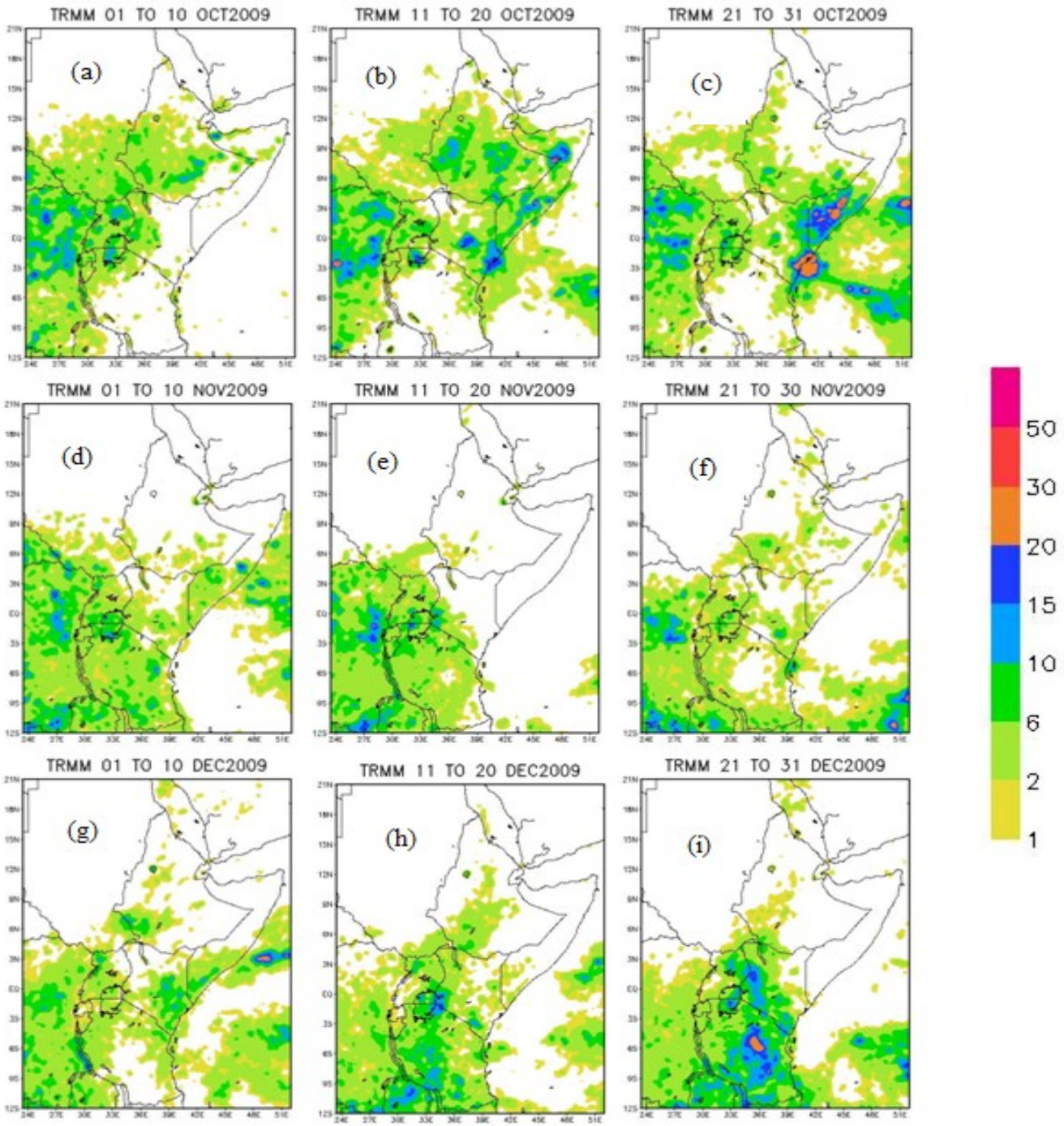

Figure 5: Spatial distribution of observed (TRMM) 10 day mean rainfall (mm/day) over the GHA region during the months of October to December 2009

Figure 6 shows the distribution of observed (TRMM) 10 day mean rainfall (in mm/day) over the GHA region during the months of October to December 2010. An almost similar pattern is again noted as was the case with 2008 and 2009 dekads. Rainfall amounts greater than 10mm/day were recorded in Central highlands of Kenya (Figure 6 d) and Central Tanzania (Figure 6 g).

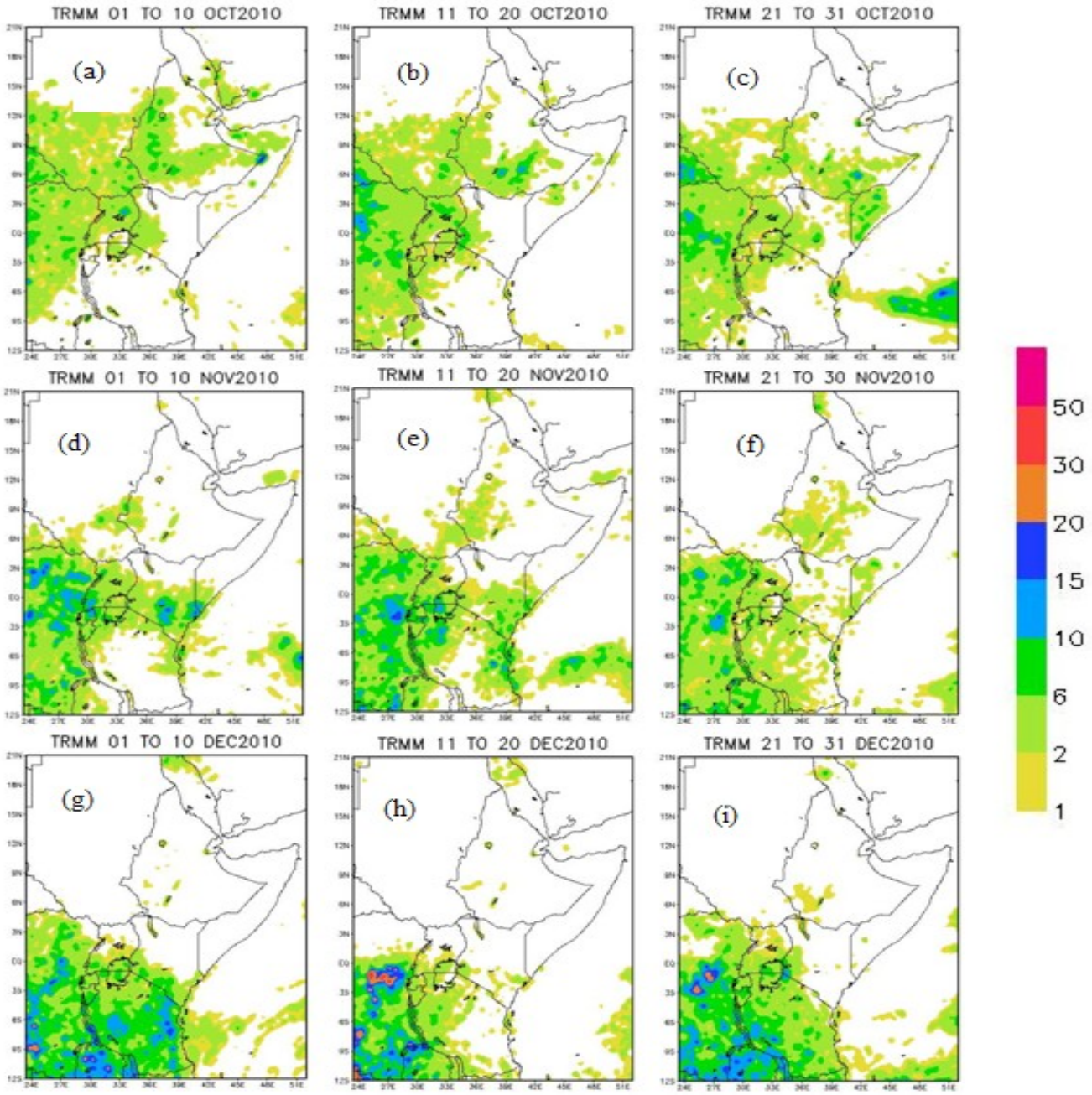

Figure 6: Spatial distribution of observed (TRMM) 10 day mean rainfall (mm/day) over the GHA region during the months of October to December 2010

Figure 7 shows the spatial distribution of the observed (TRMM) monthly mean rainfall over the GHA region during the months of October to December 2008 to 2010. The pattern shows that the TRMM rainfall estimates is consistent with the North to South migration of the ITCZ during the period with wet activities concentrated northwards and at the equator at the beginning of the October month (Figure 7 a, b, and c) and southwards towards the end of the season (Figure 7 g, h, and i).

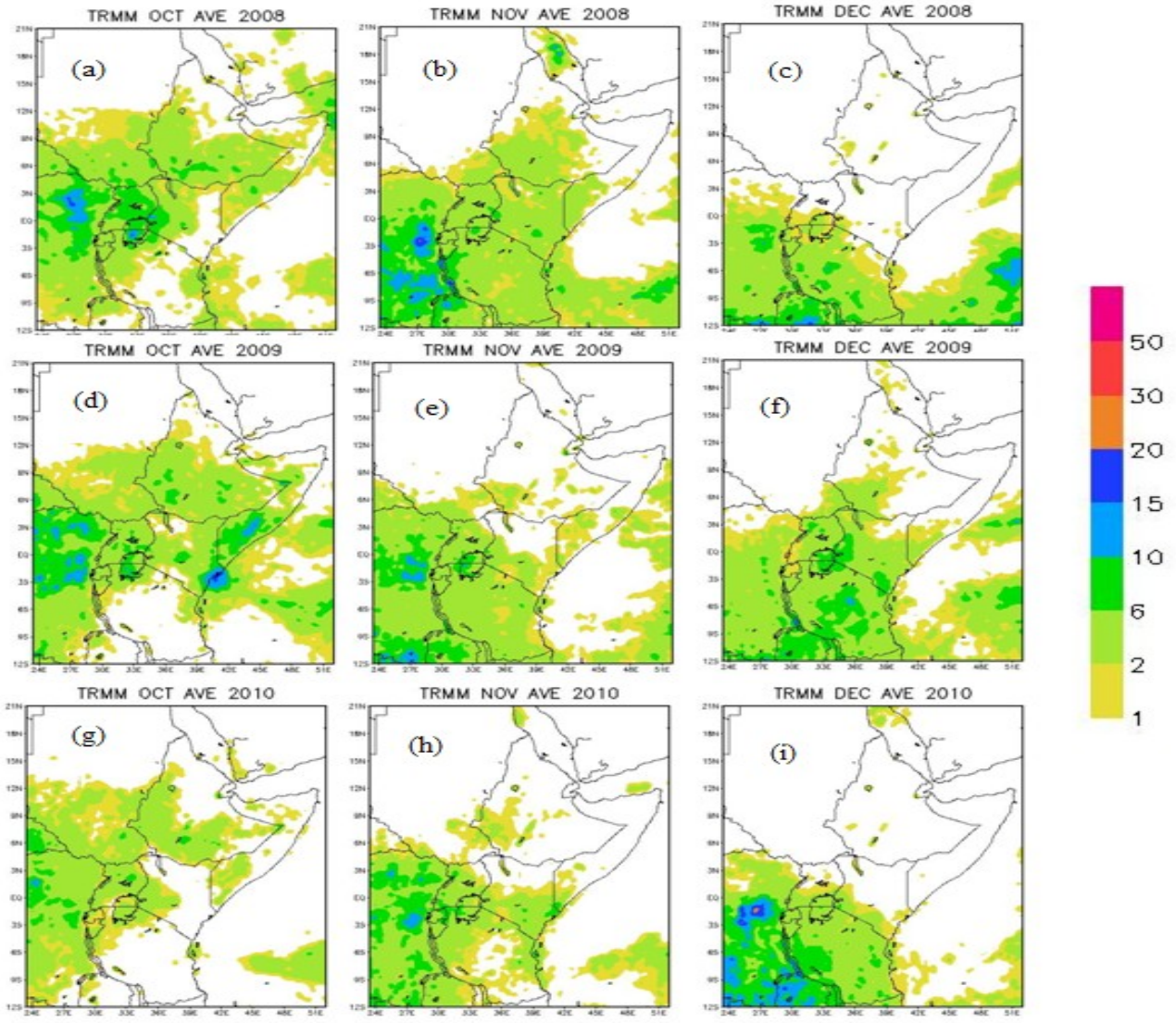

Figure 7: Spatial distribution of observed (TRMM) monthly mean rainfall over the GHA region during the months of October to December 2008, 2009 and 2010

Figure 8 shows the time series plots of observed (TRMM) daily rainfall over the GHA region for the October to December 2012 for some selected stations in the region. Wet conditions were experienced over the south-western parts of the equatorial sector represented by Entebbe, Kigoma and Dagoretti stations during the months of October and November 2012 with a maximum recorded amount of 62 mm/day recorded in Kigoma. Khartoum station which is in the northern part of the region remained dry for the entire season.

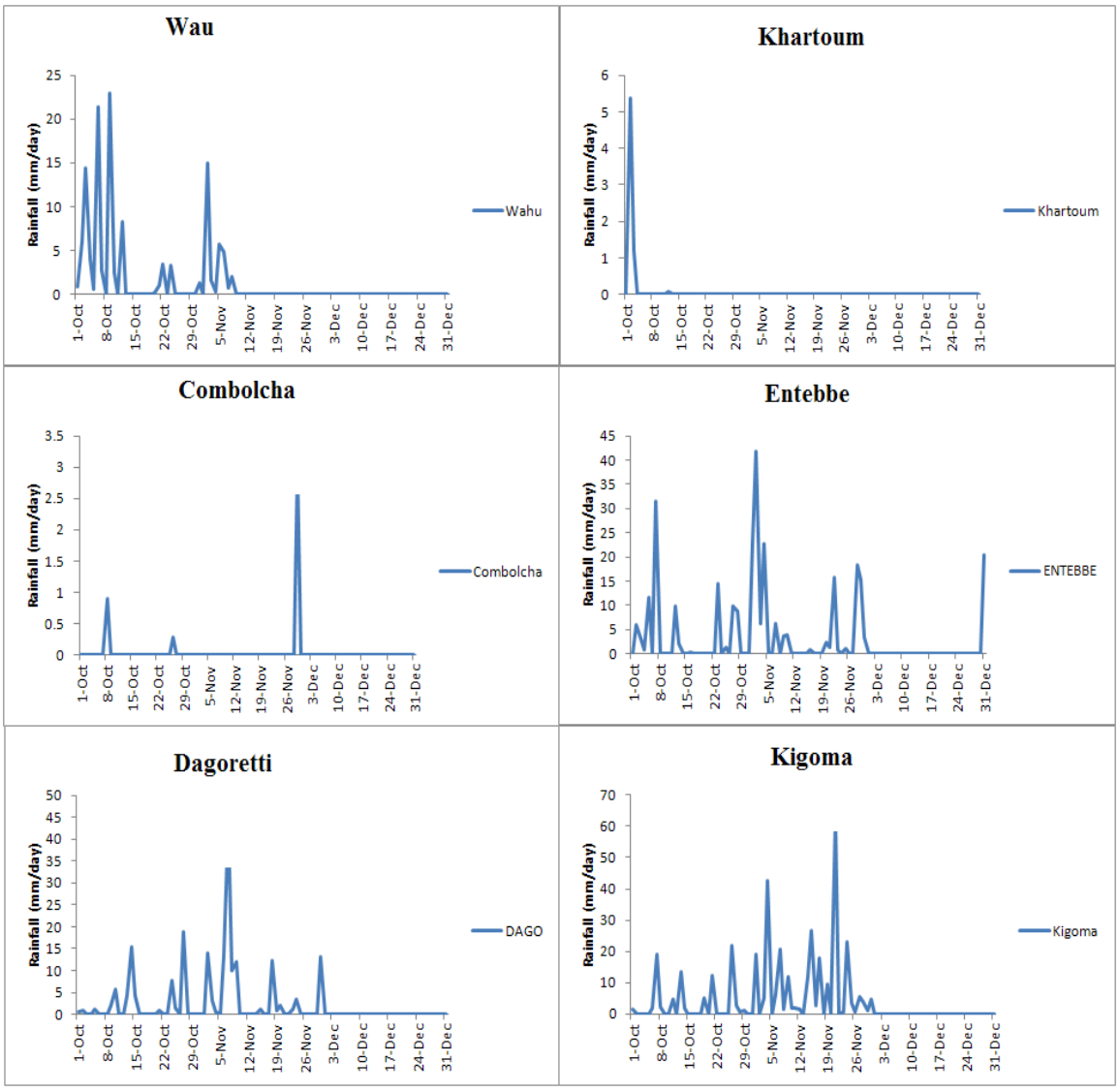

Figure 8: Time series plots showing the overall distribution of observed (TRMM) rainfall over the GHA region for the October-December 2012 for some selected stations

From the assessment of the spatial and temporal patterns of the observed (TRMM) precipitation, it is clear that rainfall distribution exhibits a Southward shift in precipitation with a marked shift in the month of December. This is consistent with the temporal and spatial pattern of the ITCZ, the main rain bearing synoptic system across the tropical Africa. OND is the season where the ITCZ migrates towards the South. During this period, the zone has both the Meridional and Zonal arms with Meridional arm responsible for the East –West variation of precipitation in the region. The intensity of Westerlies also determines the advection of the Congo air mass which is a very important rain bearing system in the region. Presences of tropical cyclones in the South West Indian Ocean also affect the rainfall distribution in both space and time. Depending on their location, intensity and track, they act to either enhance or suppress the rains. Localized features like water bodies e.g. Lake Victoria and orography also played a big role in the observed rainfall trends and patterns.

4.2 Representativeness of TRMM Rainfall Estimates over some stations in the Greater Horn of Africa region

This section utilized correlation and RMSE scores to present the performances of the TRMM rainfall estimates that was used in this study. The findings of RMSE and correlation coefficients over some stations in Kenya and Uganda during the month of October, November and December, 2012 are presented in Figure 9 and Tables 2 and 3.

The results showed RMSE values in the range of 0.8 to 10 mm/day for the October month and 6 to 20 mm/day for the November month. On average, Figure 9 shows that the values of RMSE were highest for the month of November with a RMSE value of 20 mm/day.

Correlation coefficient values were fairly good over most stations indicating significant correlations between the TRMM and observed rainfall during most of the months. The highest correlation values were recorded for the month of October 2012 in Dagoretti, Lamu and Voi with values of 0.889, 0.794 and 0.904 respectively. This corresponded with the lowest RMSE values of 2.368217, 5.036191 and 0.672204 mm/day. The shaded values in table 2 give the significant correlation scores tested at 95% confidence level.

In conclusion, the results from both RMSE and correlation analysis indicated that TRMM precipitation is a fairly good representation of observed rainfall over the selected stations. However, future analysis should strive to incorporate more of in-situ observations.

Table 2: Correlation coefficient values for the month of October, November and October, November and December (OND) season 2012 between the TRMM rainfall estimates and actual observations for some selected stations in the Greater Horn of Africa. Green shading represents positive significant correlation coefficients at 95% confidence level

	OCTOBER CORRELATION	NOVEMBER CORRELATION	OND CORRELATION
ELDORET	0.3928	0.4165	0.2174
KAKAMEGA	0.3845	0.3110	0.1083
KISUMU	0.2523	0.6704	0.3304
NAROK	0.2432	0.6890	0.1216
DAGO	0.8892	0.2923	0.2701
LAMU	0.7944	0.3030	0.4454
VOI	0.9043	0.5945	0.5357
MOMBASA	0.4797	-0.0916	0.1920
KAMPALA	0.1546	0.2596	0.1741
JINJA	0.4518	0.5782	0.3590
ENTEBBE	-0.2165	0.1927	0.1875

Table 3: RMSE values (mm/day) for the month of October, November, December and October, November and December (OND) season 2012 between the TRMM rainfall estimates and actual observations for some selected stations in the Greater Horn of Africa

	OCTOBER RMSE	NOVEMBER RMSE	DECEMBER RMSE	OND RMSE
ELDORET	8.152	8.177	8.321	8.217
KAKAMEGA	9.306	8.022	14.709	11.094
KISUMU	10.133	11.005	16.427	12.846
NAROK	6.166	8.388	11.300	8.876
DAGO	2.368	19.752	17.462	15.227
LAMU	5.036	8.272	9.285	7.740
VOI	0.672	16.149	11.525	11.400
MOMBASA	9.614	15.803	1.6163	10.651
KAMPALA	6.841	14.360	13.949	12.189
JINJA	9.776	6.959	12.094	9.863
ENTEBBE	7.834	12.929	10.605	10.635

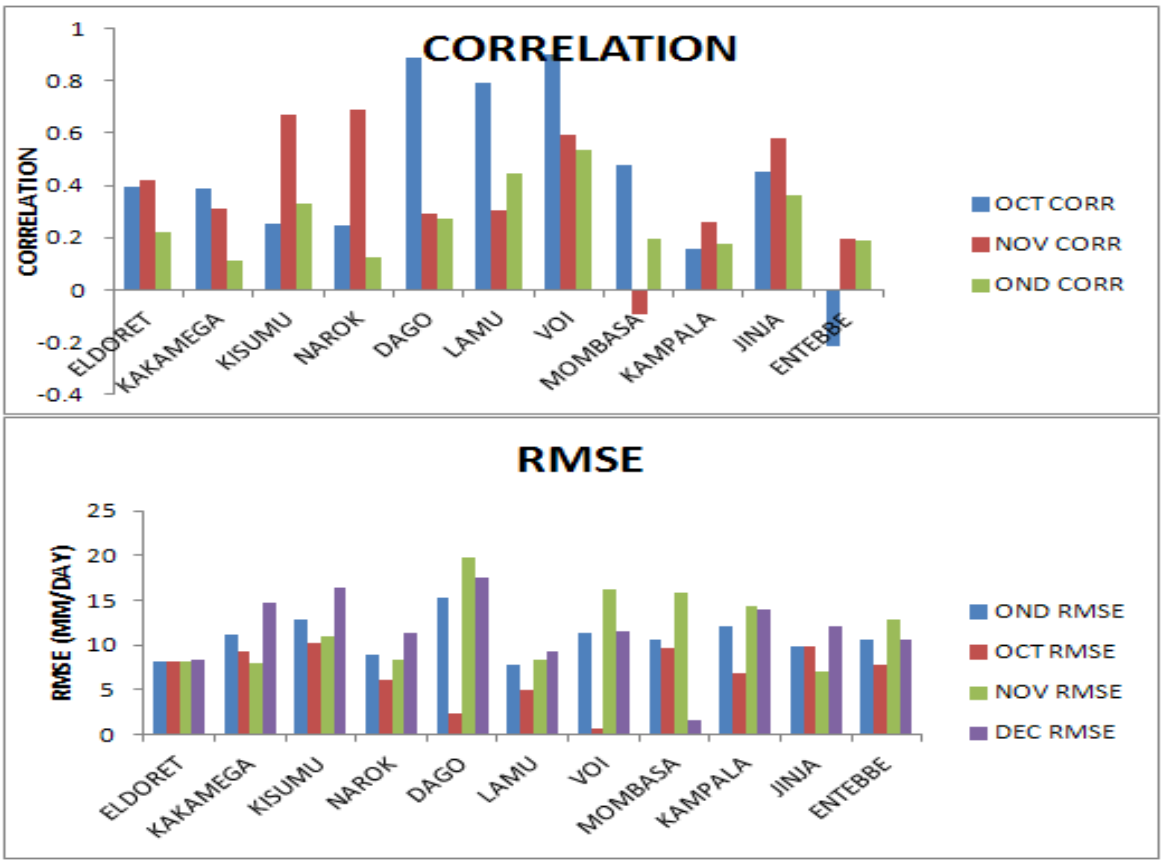

Figure 9: Correlation and RMSE analysis between the TRMM rainfall estimates and actual observations for the October, November and December 2012

4.3 Assessment of model skill and measures of accuracy

This section presents results from various statistical methodologies used to assess various skills in this research. They include RMSEs, Spatial Correlation, Bias and Equitable Threat Scores.

4.3.1 Time series plots of spatial correlation and root mean square errors for multimodels and Superensemble precipitation forecasts

Forecast datasets from TIGGE and rain rates from TRMM were used to construct a Superensemble precipitation forecast for the period 20 to 29 November, 2013. The past 450 days of multimodel forecast data of 2008 to 2012 (October, November and December) were used to train the model and calculate statistical weights. Time series of spatial correlation and RMSE scores of Multimodels and Superensemble forecasts over the Greater Horn of Africa are presented on Figure 10. These are three case runs starting at 20, 21 and 22, November 2013 respectively each with a forecast lead time of 10 days. These plots show consistently high and low spatial correlation and RMSE scores respectively for the Multimodel Superensemble forecasts as compared with that of individual models.

The RMSE of the FSU superensemble ranges from 4.8 to 8.0 mm/day (Figure 10 b and f) for all 10 days of forecasts. Irrespective of the forecast day, SE forecasts RMSE ranges have a small spread as compared with the individual multimodels. This indicates a major improvement for the forecast for all the forecast days.

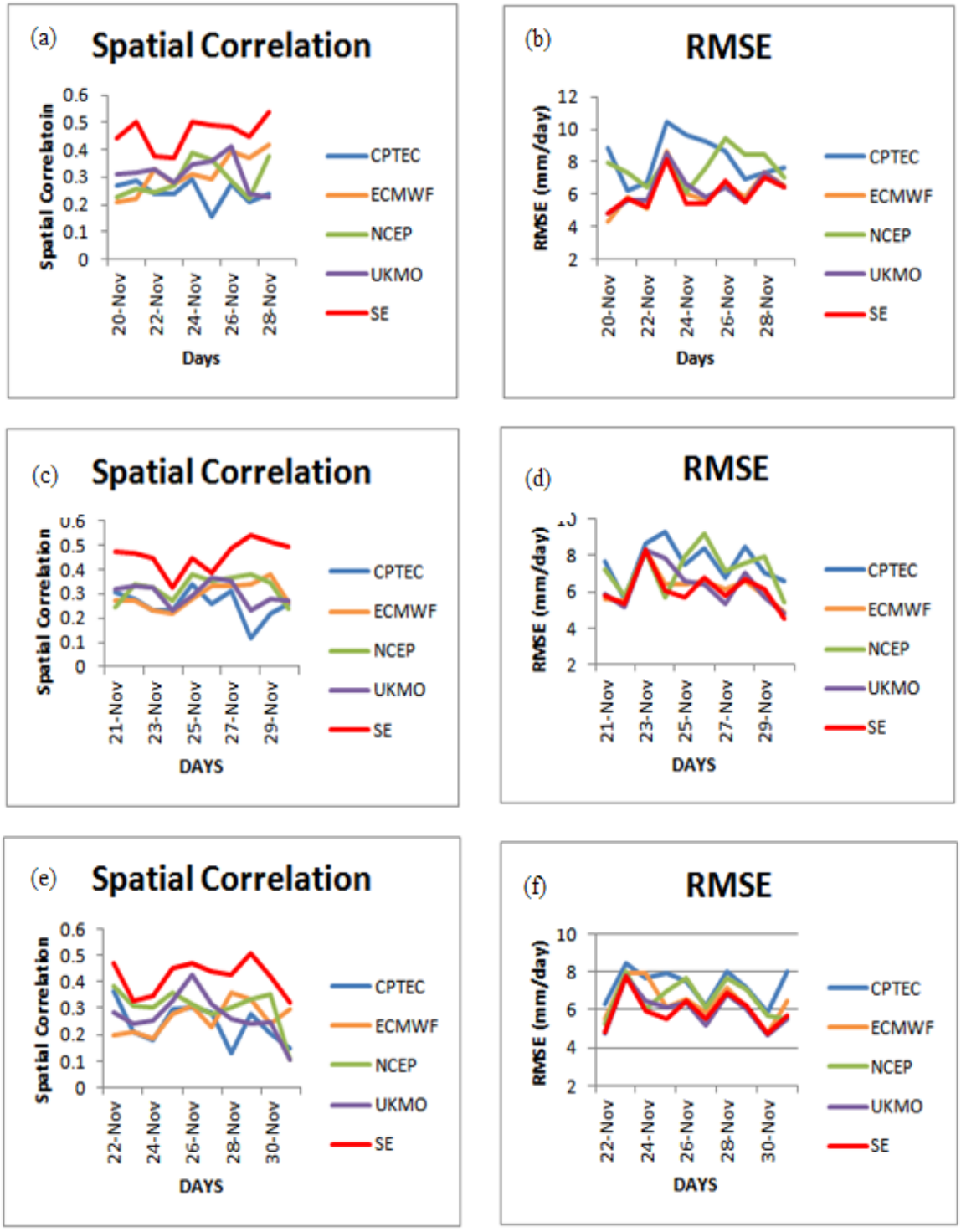

Figure 10: Time series of spatial correlation and RMSE (mm/day) scores of Multimodels and Superensemble forecasts over the Greater Horn of Africa. These are three case runs starting at 20, 21 and 22 November 2013 respectively each with lead times of 10 days

4.3.2 Spatial plots of Multimodel and Superensemble precipitation forecasts (mm/day)

In this section, observed rain, as seen from the TRMM files, the individual member model forecasts and the FSU superensemble forecasts is shown. Also included on top of each panel are the values for the Spatial Correlation and RMSE. The construction of the superensemble made it possible to achieve consistent and better scores. If the member models carry consistent and large systematic errors then the superensemble is able to capitalize on these and reduce them.

Figure 11shows spatial plots for RMSE and Spatial Correlation scores between TRMM and model outputs (individual models and SE forecasts) over the Greater Horn of Africa region for day 1 (20 November 2013) and day 2 (21 November 2013). SE forecast product for both day 1 and day 2 outperformed all the individual models in the suite with a RMSE of 4.83 mm/day and 5.75 mm/day and SC of 0.47 and 0.44 for day 1 and day 2 respectively (Figure 11 (i)b and (ii)b). CPTEC model had the highest RMSE of 8.81 mm/day (Figure 11 (i) f). CPTEC indicated that for day 1, the south western part of the region could receive rainfall amounts of up to 50 mm/day which was contrary to the observation.

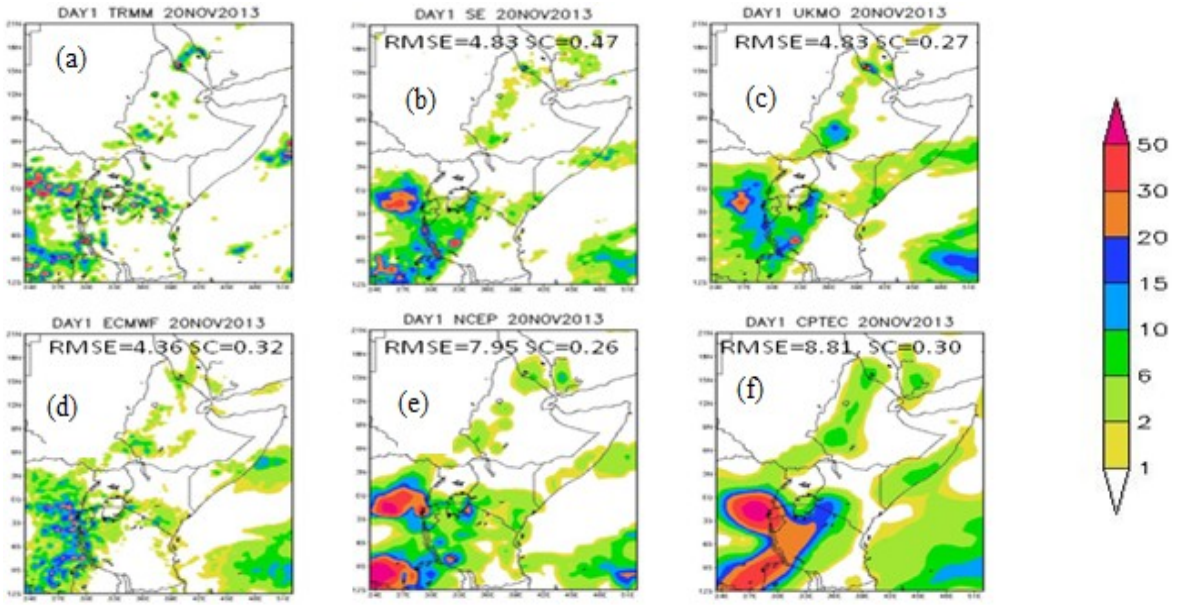

(i)

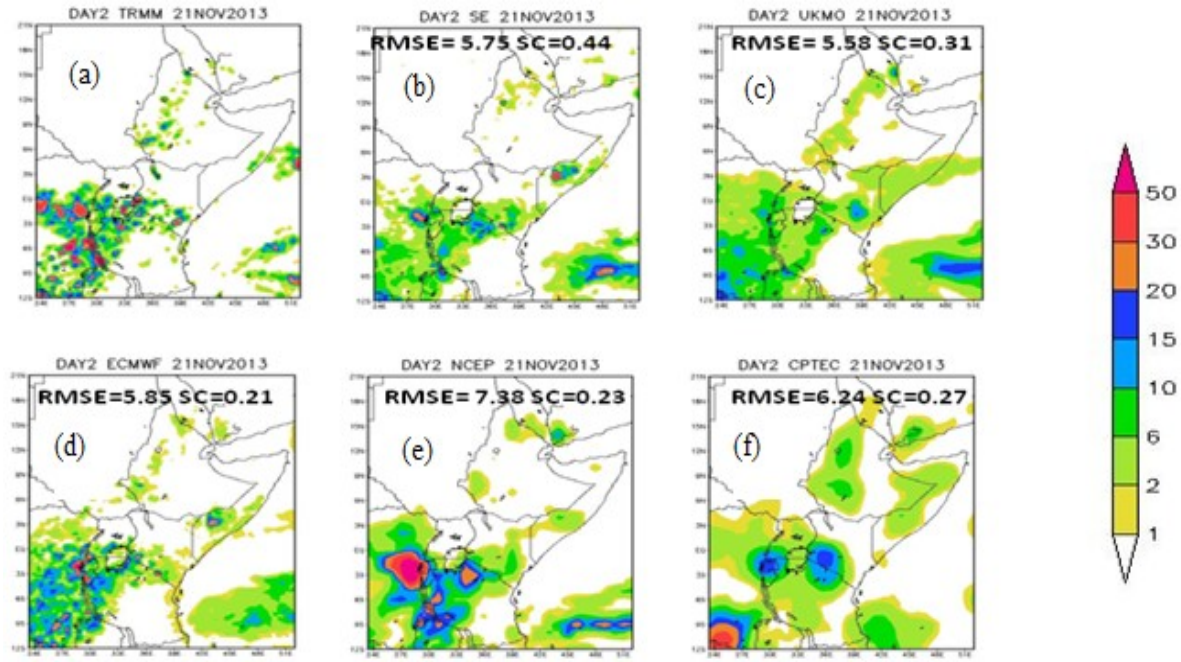

(ii)

Figure 11: Spatial Plots showing RMSE and Spatial Correlation scores between TRMM and model outputs (individual models and SE forecasts) over the Greater Horn of Africa region. (i) And (ii) Shows Plots for Day 1 (20 November 2013) and Day 2 (21 November 2013) respectively. Numbers in every forecast panels show the RMSE and SC

Figure 12 shows spatial plots for RMSE and Spatial Correlation scores between TRMM and model outputs (individual models and SE forecasts) over the Greater Horn of Africa region for day 3 (22 November 2013) and day 4 (23 November 2013). The output from ECMWF had a better RMSE of 5.14 mm/day for day 3 (Figure 12 (i) d) as compared to that from SE which had a value of 5.19 mm/day (Figure 12 (i) b). For day 4, UKMO model performed well individually with a SC and RMSE score of 0.33 and 8.57 mm/day (Figure 12 (ii) c). The SE outperformed all the models in the suite as it had the highest SC of 0.5 (Figure 12 (i) b). CPTEC model performed poorly individually with a RMSE of 10.46 mm/day for day 4 (Figure 12 (ii) f).

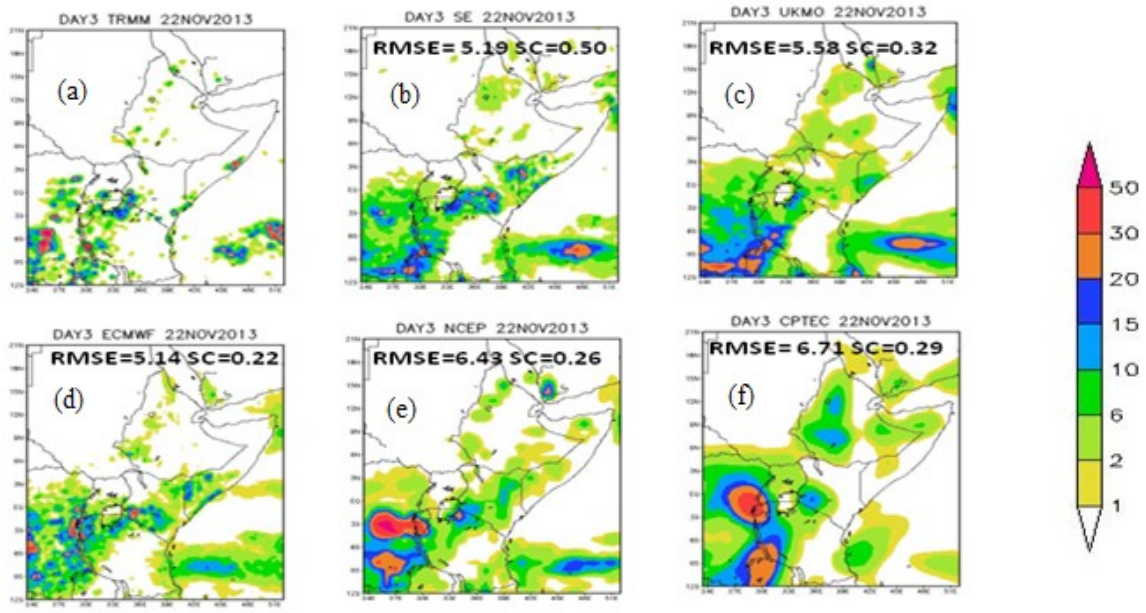

(i)

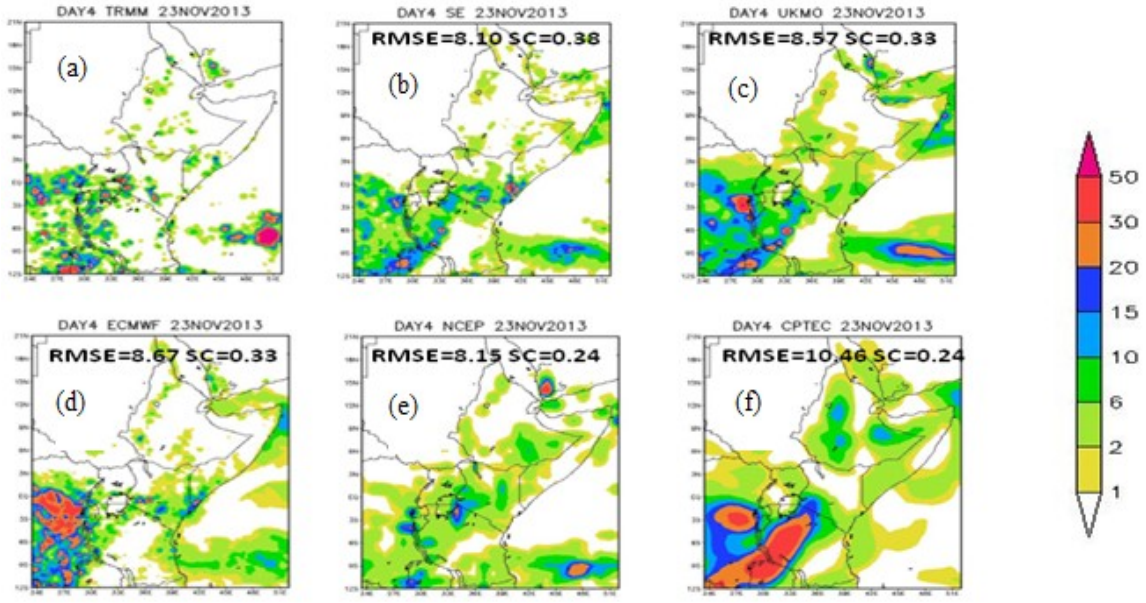

(ii)

Figure 12: Spatial Plots showing RMSE and Spatial Correlation scores between TRMM and model outputs (individual models and SE forecasts) over the Greater Horn of Africa region. (i) and (ii) Shows Plots for Day 3 (22 November 2013) and Day 4 (23 November 2013) respectively. Numbers in every forecast panels show the RMSE and SC

Spatial plots of RMSE and SC scores between TRMM and model outputs (individual models and SE forecasts) over the Greater Horn of Africa region for day 5 (24 November 2013) and day 6 (25 November 2013) are shown in Figure 13. For both day 5 and 6, the SE had superior forecasts in terms of RMSE and SC. Individually, ECMWF had a better SC and RMSE score of 0.28 and 5.99 mm/day (Figure 13 (i) d). This compares with a SE score of 0.37 and 5.43 mm/day for SC and RMSE respectively (Figure 13 (i) c). UKMO model performed better in day 6 with a SC and RMSE score of 0.34 and 5.82 mm/day (Figure 13 (ii)c) with SE scores of 0.50 and 5.41 mm/day for the same day (Figure 13 (ii)b). CPTEC model performed poorly individually with SC and RMSE scores of 0.24 and 9.64 mm/day for day 5 (Figure 13 (i) f) and 0.29 and 9.22 mm/day for day 6 (Figure 13 (ii) f).

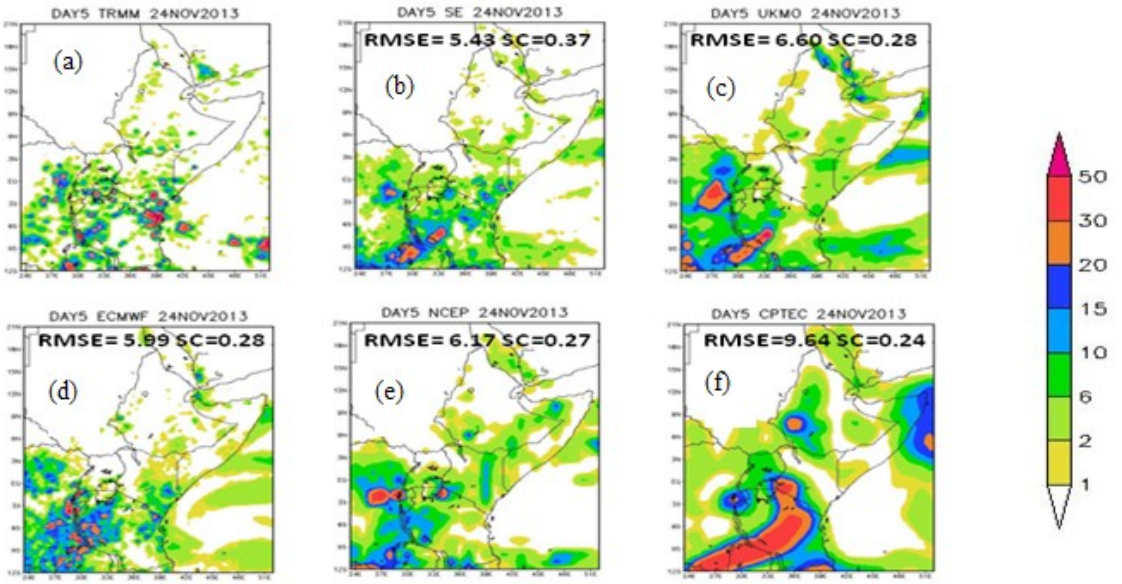

(i)

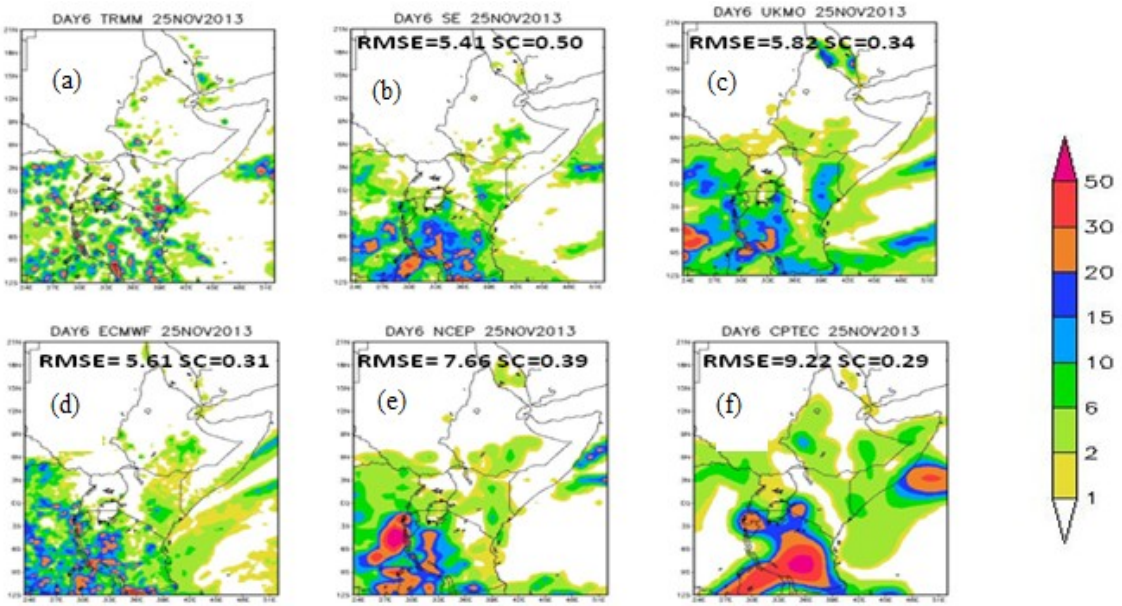

(ii)

Figure 13: Spatial Plots showing RMSE and Spatial Correlation scores between TRMM and model outputs (individual models and SE forecasts) over the Greater Horn of Africa region. (i) and (ii) Shows Plots for Day 5 (24 November 2013) and Day 6 (25 November 2013) respectively. Numbers in every forecast panels show the RMSE and SC

Figure 14 shows spatial plots for RMSE and Spatial Correlation scores between TRMM and model outputs (individual models and SE forecasts) over the Greater Horn of Africa region for day 7 (26 November 2013) and day 8 (27 November 2013). Again, the SE forecast gave better results than the individual models as were seen in the SC and RMSE scores. The TRMM showed an intensification of rainfall activities in the south western part of the region and most of it was captured by the SE and ECMWF model. Individually, UKMO model had a better SC and RMSE score for both day 7 and 8 of 0.36 and 6.46 mm/day and 0.41 and 5.50 mm/day respectively (Figure 14 (i) c and Figure 14 (ii) c). This compares with a SE score of 0.49 and 6.88 mm/day for day 7 and 0.48 and 5.56 mm/day for day 8 for SC and RMSE respectively (Figure 14 (i) b and Figure 14 (ii) b).

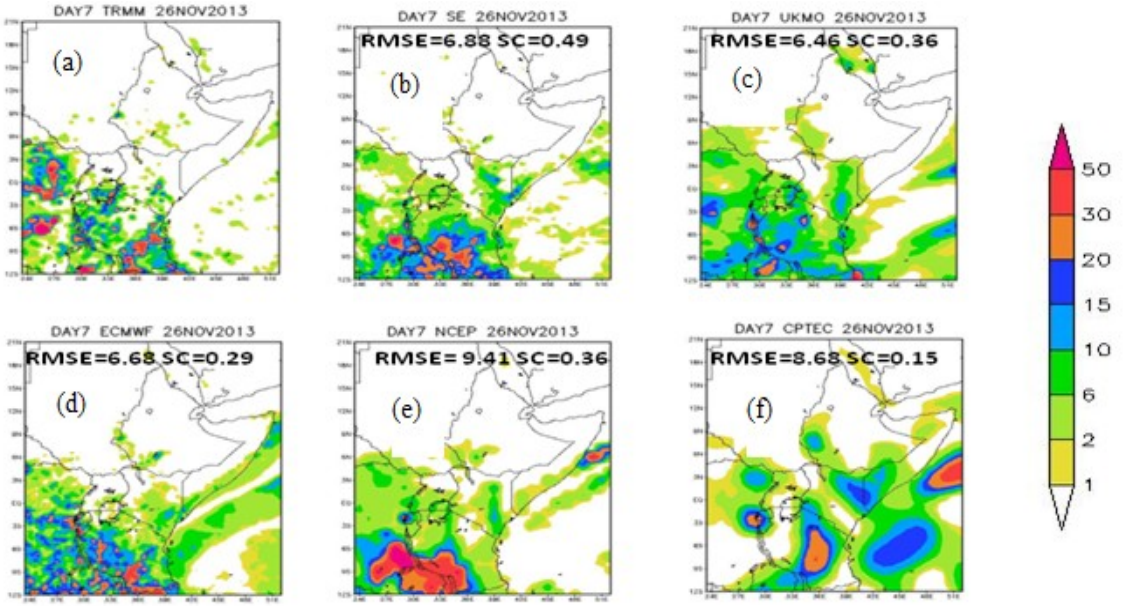

(i)

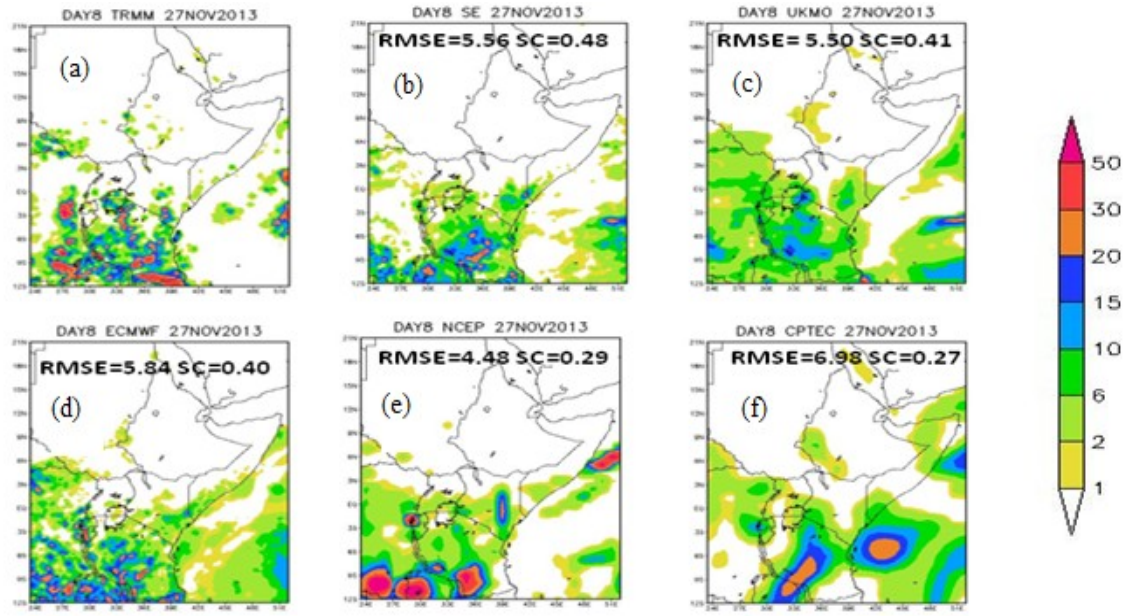

(ii)

Figure 14: Spatial Plots showing RMSE and Spatial Correlation scores between TRMM and model outputs (individual models and SE forecasts) over the Greater Horn of Africa region. (i) and (ii) Shows Plots for Day 7 (26 November 2013) and Day 8 (27 November 2013) respectively. Numbers in every forecast panels show the RMSE and SC

Figure 15 shows spatial plots for RMSE and Spatial Correlation scores between TRMM and model outputs (individual models and SE forecasts) over the Greater Horn of Africa region for day 9 (28 November 2013) and day 10 (29 November 2013). In terms of the SC and RMSE, the SE had better scores. TRMM pattern for day 9 forecast showed a reduction of rainfall activities from the previous day (day 8) in the south western part of the region. Individually, ECMWF model had a better SC and RMSE score for both day 9 and 10 of 0.37 and 7.35 mm/day and 0.42 and 6.49 mm/day respectively (Figure 15 (i) d and Figure 15 (ii) d). This compares with a SE score of 0.45 and 7.02 mm/day for day 9 and 0.54 and 6.42 mm/day for day 10 for SC and RMSE respectively (Figure 15 (i) b and Figure 15 (ii) b). In summary, the superensemble carried consistent and better values for these skills through Day 10 of forecasts as compared to the individual models.

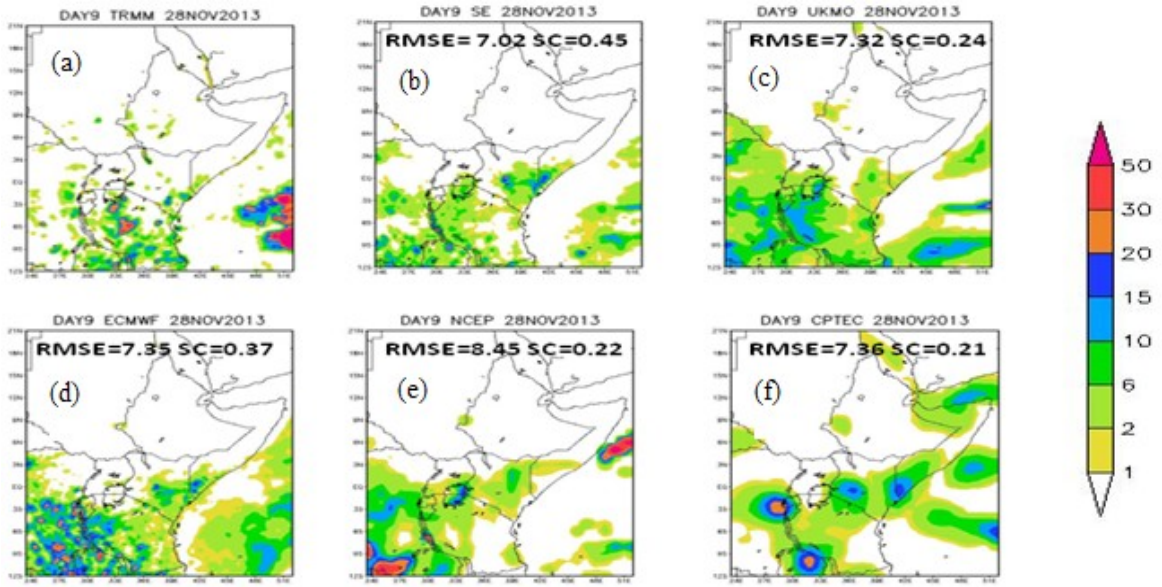

(i)

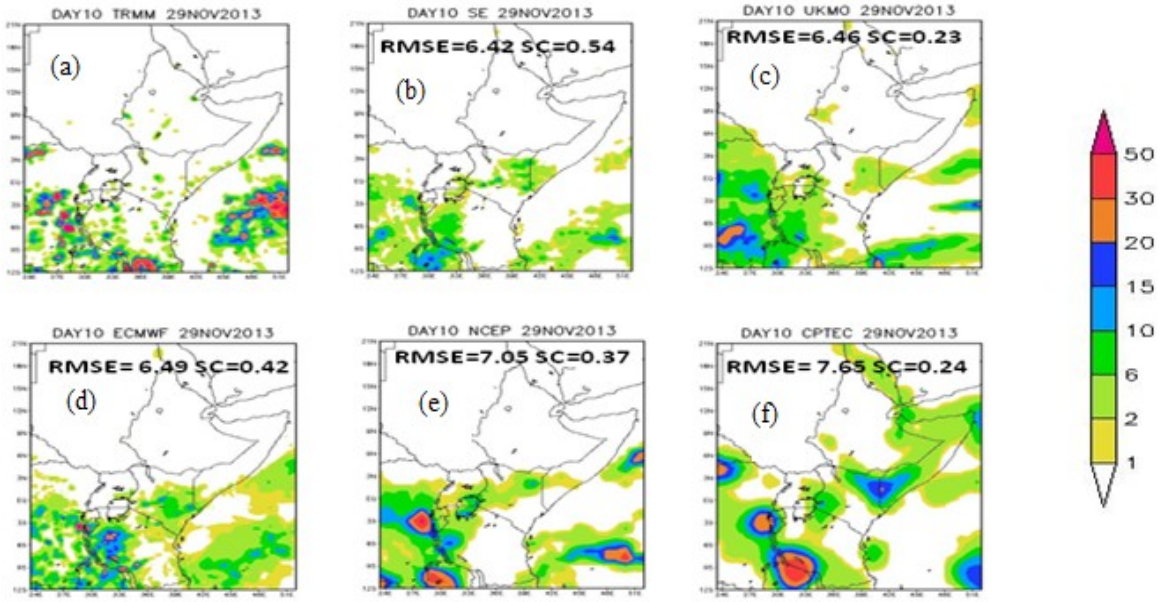

(ii)

Figure 15: Spatial Plots showing RMSE and Spatial Correlation scores between TRMM and model outputs (individual models and SE forecasts) over the Greater Horn of Africa region. (i) and (ii) Shows Plots for Day 9 (28 November 2013) and Day 10 (29 November 2013) respectively. Numbers in every forecast panels show the RMSE and SC

Table 4 shows the Comparison between the best of the four individual models participating in the superensemble suite and the Superensemble (SE) forecast in terms of spatial correlation and RMSE scores. It is noted that for all the forecast days, the UKMO and ECMWF performed better individually as compared to other individual models in the suite.

Table 4: Comparison between the best of four individual models participating in the superensemble suite and the Superensemble (SE) forecast in terms of Spatial Correlation and RMSE scores

Day	Model	Correlation coefficient	RMSE (mm/day)
1	SE	0.47	4.83
	ECMWF	0.32	4.36
2	SE	0.44	5.75
	UKMO	0.31	5.58
3	SE	0.50	5.19
	UKMO	0.32	5.58
4	SE	0.38	8.10
	ECMWF	0.33	8.67
5	SE	0.37	5.43
	ECMWF	0.28	5.89
6	SE	0.50	5.41
	NCEP	0.39	7.66
7	SE	0.49	6.88
	UKMO	0.36	6.46
8	SE	0.48	5.56
	UKMO	0.41	5.60
9	SE	0.45	7.02
	ECMWF	0.37	7.35
10	SE	0.54	6.42
	ECMWF	0.42	6.49

4.3.3 Equitable Threat Scores and bias scores for different thresholds

Equitable Threat Scores (ETS) and Bias scores were computed for the precipitation forecasts for all the models for each day of forecast over the region, i.e. Day 1 to 10 for different thresholds. For this study, arbitrary thresholds of 0.2, 2, 5, 10, 25, 35 and 50 mm/day were chosen.

Figure 16 shows ETS and Bias scores for Day 1(20 Nov. 2013), Day 2 (21 Nov. 2013) and Day 3 (22 Nov. 2013) forecasts of FSU multimodel superensemble and the individual models forecasts over the Greater Horn of Africa region. Left and right panels are ETS and Bias scores respectively. The abscissas in these diagrams are the rainfall rate thresholds, for instance, number 5 denotes all rainfall in excess of 5 mm/day. The ordinate denotes the ETS in the left panels and the bias scores in the right panels. The Day 1 ETS for most member models ranges from 0.133 (CPTEC) to 0.279 (UKMO) for 0.2 mm/day threshold and 0.142 (CPTEC) to 0.262 (UKMO/ECMWF). This compares with superensemble ETS values of 0.308 and 0.274 for 0.2 and 2 mm/day thresholds respectively. The day 1 bias for most member models ranges from 1.962 (UKMO) to 2.784 (CPTEC) for 0.2 mm/day threshold and 1.56 (ECMWF) to 2.935 (CPTEC) for 2 mm/day threshold. This compares with superensemble bias scores of 1.348 and 1.451 for 0.2 and 2 mm/day thresholds respectively. Forecasts from NCEP model had a tendency to over-forecast at precipitation thresholds greater than 10 mm/day.

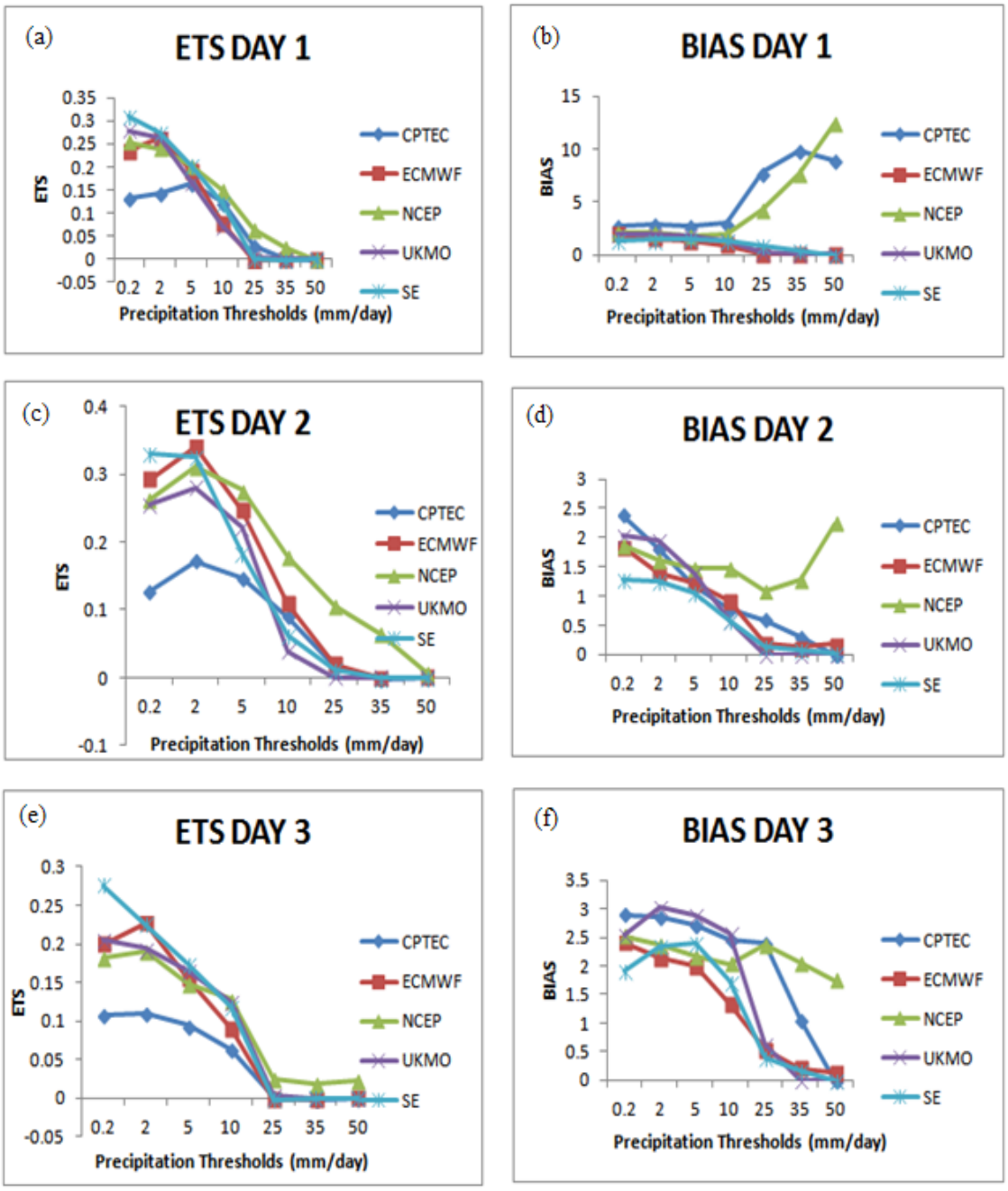

Figure 16: Equitable Threat Score (ETS) and Bias scores for Day 1(20 Nov. 2013), Day 2 (21 Nov. 2013) and day 3 (22 Nov. 2013) forecasts of FSU multimodels over the Greater Horn of Africa region. Left and right panels are ETS and Bias scores respectively

Figure 17 shows ETS and Bias scores for Day 4(23 Nov. 2013), Day 5 (23 Nov. 2013) and Day 6 (25 Nov. 2013) forecasts of FSU multimodel superensemble and the individual models forecasts. Forecast from CPTEC model had the lowest ETS score of 0.083 at Day 5 while NCEP and ECMWF models performed better individually with ETS scores of 0.202 (Day 5) and 0.298 (Day 6) respectively for precipitation thresholds of 0.2 and 2 mm/day. This compares with slightly better score of 0.334 (Day 6) for the superensemble forecast at the same thresholds. All the models had a tendency to over-forecast precipitation as they had Bias scores greater than one with the highest bias score of 2.44 (Day 5) for CPTEC model. Superensemble forecast had a superior bias score of 1.138 (Day 6).

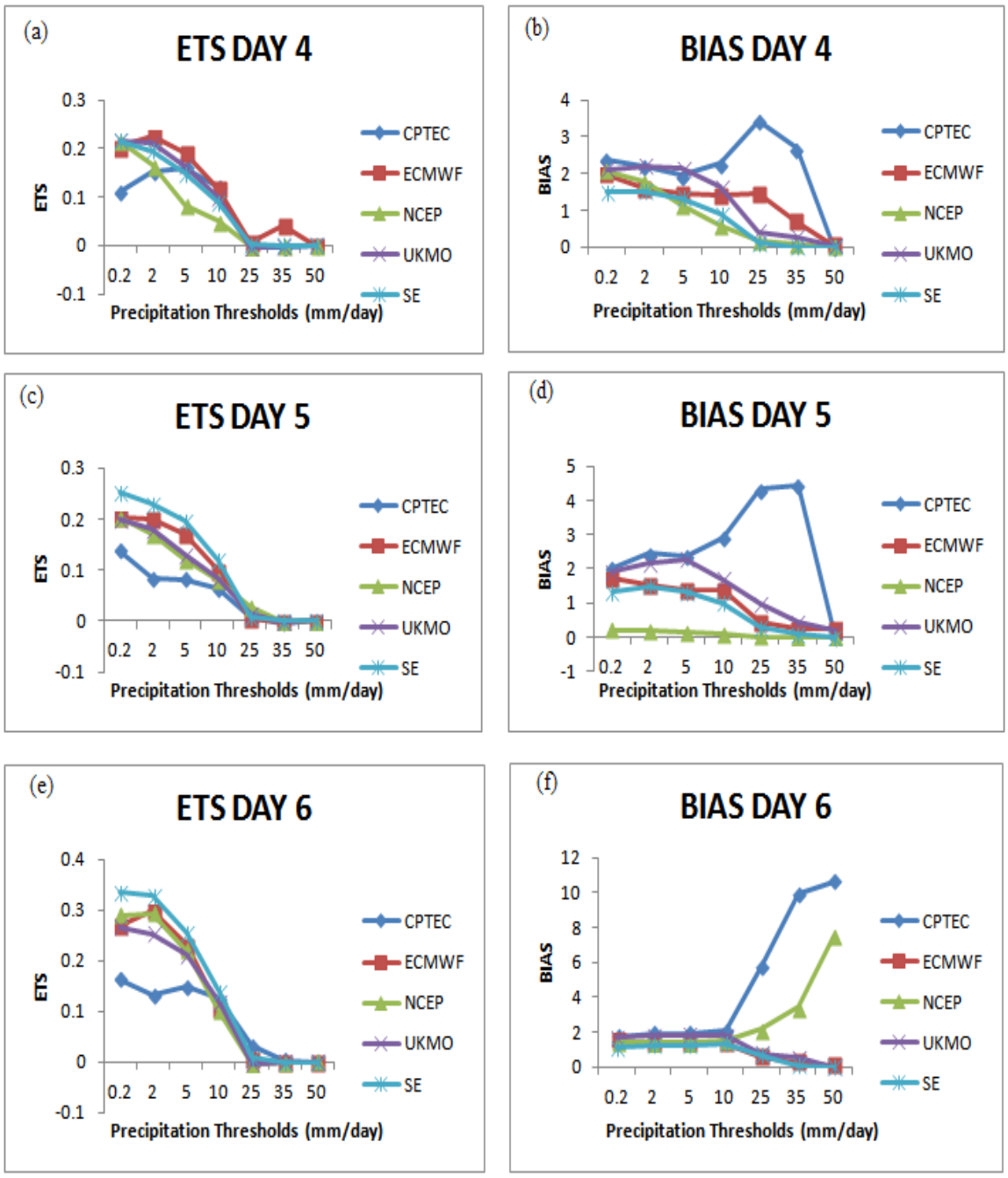

Figure 17: Equitable Threat Score (ETS) and Bias scores for Day 4(23 Nov. 2013), Day 5 (24 Nov. 2013) and day 6 (25 Nov. 2013) forecasts of FSU multimodels over the Greater Horn of Africa region. Left and right panels are ETS and Bias scores respectively

Figure 18 shows ETS and Bias scores for Day 7(26 Nov. 2013), Day 8 (27 Nov. 2013), Day 9 (28 Nov. 2013) and Day 10 (29 Nov. 2013) forecasts of FSU multimodel superensemble and the individual models forecasts. All the models had Bias scores greater than one with the highest bias score of 2.233 (Day 9) for CPTEC model. Superensemble forecast however had a superior bias score of 1.01 (Day 8). At precipitation thresholds greater than 10 mm/day, NCEP model had a tendency to over-forecast precipitation with a bias of up to 9 (Day 8). NCEP and ECMWF models performed better individually for all the thresholds. The best ETS score of 0.353 (Day 7) was recorded for the superensemble forecast.

The question is how good is an ETS in this range? That is the current now casting skill for most global operational models. This score does signify some degree of usefulness of forecast over a large-scale model whose horizontal resolution is of the order of 100 km. This skill cannot be directly compared to that of mesoscale models.

Another aspect, we see here is that the skills for light rains, i.e. thresholds less than 10 mm/day are predicted with better skills by the multimodel superensemble and even the individual models. This is due to the nature of the consistent systematic errors of the member models which are easily exploited by the multimodel superensemble in its forecasts. However, thresholds greater than 10 mm/day are predicted with lower skills by the multimodel superensemble and even the individual models.

It is seen from these figures that individual models carry large bias errors which are very much improved by the multimodel superensemble.

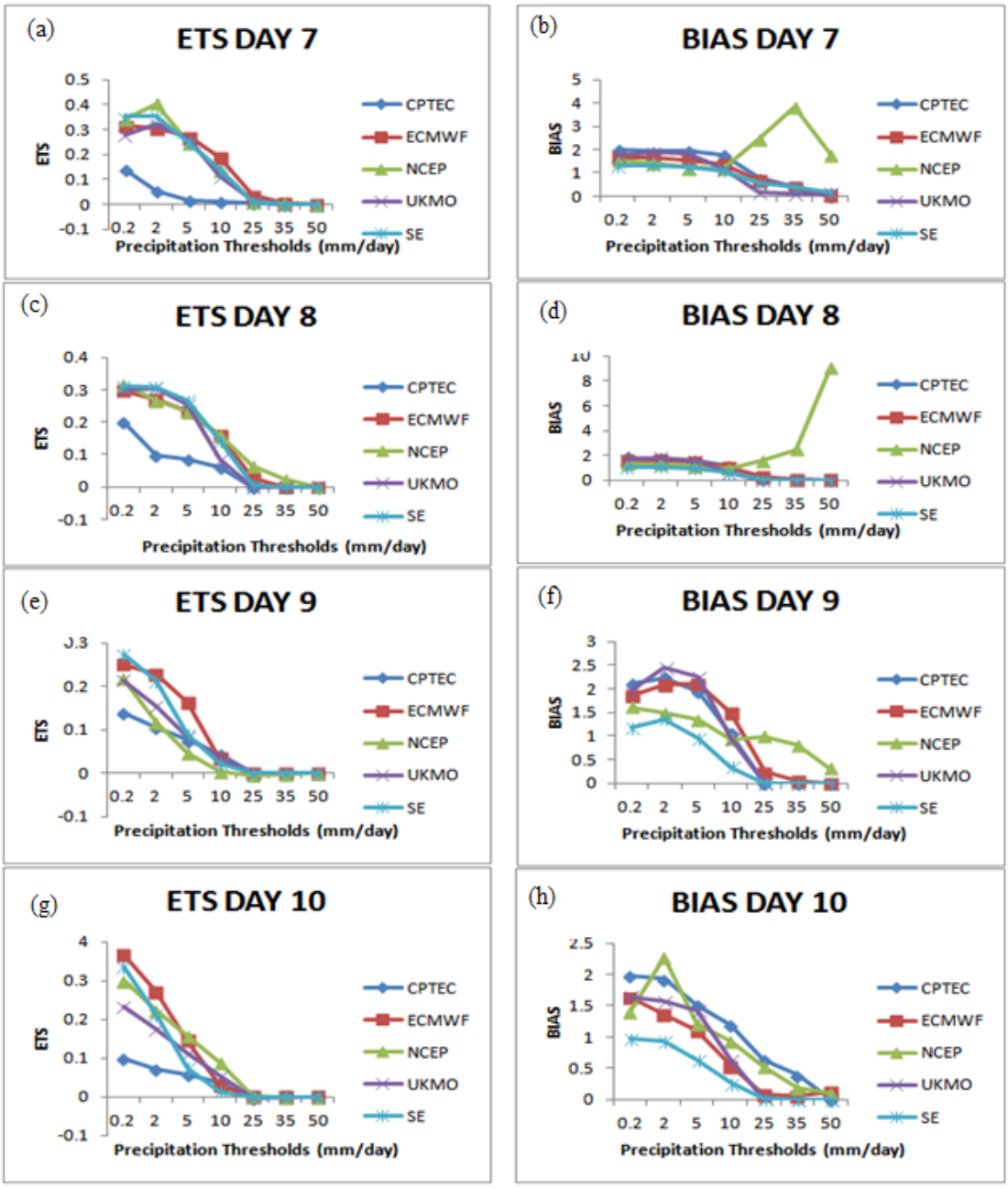

Figure 18: Equitable Threat Score (ETS) and Bias scores for Day 7(26 Nov. 2013), Day 8 (27 Nov. 2013), Day 9 (28 Nov. 2013) and day 10 (29 Nov. 2013) forecasts of FSU multimodels over the Greater Horn of Africa region. Left and right panels are ETS and Bias scores respectively

Table 5 and 6 shows the ETS and bias for each individual model and superensemble forecasts for all the forecast days for thresholds of 0.2, 2 and 5 mm/day. ECMWF and UKMO performed better individually in terms of ETS and bias scores. The superensemble however outperformed all the individual models.

Table 5: Equitable Threat Scores for each individual model and superensemble forecasts for 0.2, 2 and 5 mm/day thresholds for all the forecast days

		DAY									
Model	Thresholds (mm/day)	1	2	3	4	5	6	7	8	9	10
SE	0.2	0.308	0.33	0.276	0.216	0.251	0.334	0.352	0.311	0.273	0.335
	2	0.274	0.325	0.225	0.195	0.23	0.33	0.353	0.307	0.212	0.211
	5	0.203	0.184	0.173	0.149	0.197	0.255	0.248	0.267	0.09	0.075
CPTEC	0.2	0.133	0.128	0.107	0.112	0.138	0.163	0.137	0.2	0.138	0.1
	2	0.142	0.172	0.109	0.154	0.083	0.131	0.055	0.097	0.105	0.07
	5	0.163	0.146	0.094	0.161	0.082	0.148	0.018	0.087	0.076	0.057
ECMWF	0.2	0.236	0.292	0.2	0.203	0.202	0.27	0.315	0.297	0.25	0.368
	2	0.262	0.34	0.227	0.224	0.201	0.298	0.305	0.27	0.228	0.27
	5	0.194	0.247	0.155	0.191	0.17	0.231	0.272	0.232	0.162	0.144
NCEP	0.2	0.254	0.263	0.182	0.214	0.202	0.29	0.341	0.314	0.217	0.301
	2	0.24	0.311	0.19	0.165	0.171	0.292	0.404	0.266	0.118	0.223
	5	0.203	0.277	0.148	0.083	0.121	0.22	0.246	0.235	0.047	0.158
UKMO	0.2	0.279	0.255	0.205	0.216	0.198	0.266	0.277	0.3	0.214	0.232
	2	0.262	0.28	0.194	0.211	0.178	0.253	0.32	0.305	0.153	0.173
	5	0.167	0.221	0.165	0.164	0.13	0.212	0.264	0.253	0.082	0.111

Table 6: Bias scores for individual models and superensemble forecasts for 0.2, 2 and 5 mm/day thresholds for all the forecast days

		DAY									
Model	Thresholds (mm/day)	1	2	3	4	5	6	7	8	9	10
SE	0.2	1.348	1.272	1.927	1.499	1.326	1.138	1.301	1.01	1.186	0.976
	2	1.451	1.254	2.344	1.52	1.492	1.245	1.326	1.092	1.362	0.943
	5	1.475	1.064	2.4	1.335	1.324	1.274	1.247	0.97	0.956	0.633
CPTEC	0.2	2.784	2.382	2.894	2.393	2.023	1.77	1.986	1.822	2.102	1.976
	2	2.935	1.814	2.85	2.211	2.444	1.932	1.919	1.727	2.233	1.93
	5	2.782	1.171	2.716	1.947	2.379	1.955	1.931	1.546	1.947	1.515
ECMWF	0.2	1.993	1.838	2.408	1.967	1.71	1.533	1.666	1.603	1.869	1.632
	2	1.56	1.406	2.135	1.583	1.538	1.347	1.67	1.607	2.095	1.371
	5	1.294	1.239	2.004	1.454	1.386	1.35	1.545	1.45	2.102	1.107
NCEP	0.2	2.1	1.858	2.522	2.058	0.198	1.431	1.534	1.337	1.607	1.403
	2	2.07	1.604	2.372	1.772	0.178	1.387	1.447	1.289	1.487	2.268
	5	1.86	1.486	2.177	1.119	0.13	1.403	1.238	1.124	1.347	1.207
UKMO	0.2	1.962	2.027	2.548	2.112	1.911	1.706	1.791	1.654	1.962	1.646
	2	1.94	1.956	3.02	2.2	2.148	1.795	1.861	1.821	2.449	1.57
	5	1.835	1.395	2.89	2.126	2.29	1.834	1.816	1.584	2.264	1.418

CHAPTER FIVE

5.0 CONCLUSIONS AND RECOMMENDATIONS

This chapter provides conclusions drawn from the results and recommendations for further work.

5.1 Conclusions

This study was carried out to investigate the predictability of daily precipitation over the Greater Horn of Africa region using the multimodel Superensemble technique. The multimodel superensemble contains training and a forecast phase. During the training phase, statistical weights are generated based on recent past performances of the member models and their collective bias errors are minimized by this procedure. Statistical weights for each day of forecast were prepared recognizing that some models are more skillful early on in their forecasts, whereas some models carry more skills later in their forecasts.

A large suite of large scale global models from the THORPEX Interactive Grand Global Ensemble (TIGGE) archive were used to examine the state of the art skills through Day 10 of forecasts for precipitation over the Greater Horn of Africa belt. They include European Centre for Medium Range Weather Forecasts (ECMWF), National Centre for Environmental Prediction (NCEP), Center for Weather Forecast and Climatic Studies (CPTEC) and United Kingdom Meteorological Office (UKMO).

From the assessment of the spatial and temporal patterns of the observed (TRMM) precipitation, it is clear that rainfall distribution exhibits a Southward shift in precipitation with a marked shift in the month of December. This is consistent with the temporal and spatial pattern of the ITCZ, the main rain bearing synoptic system across the tropical Africa.

The construction of the superensemble did provide the best product in terms of RMS error and spatial correlations for each of the forecast days. The superensemble forecasts showed skill scores much higher than both the ensemble mean and the best performing

model in the suit. For example, equitable threat scores and bias scores for all forecasts for the region carried the best scores close to 1.0.

The superensemble is thus a robust technique that can improve the geographical location and even the amplitude of the predicted rains as trained and validated with the blended TRMM product resolution. The systematic errors in the geographical locations of the rains are much improved by the superensemble. The amplitude of the predicted rains is corrected towards the TRMM based estimates by this procedure.

The multimodel superensemble technique is therefore a feasible proposition in real time forecasting that can be implemented in the Greater Horn of Africa region as one of the forecasting tool.

5.2 Recommendations

Further work in multimodel superensemble forecasting is possible from a suite of mesoscale high resolution models. A superensemble forecasts based on mesoscale models would be more suitable and would improve future versions of superensemble forecast products.

In this research, satellite rainfall estimates were used as the analysis fields. Future research in the region should endeavor to incorporate the real station observed data as it gives what actually happened. Blending of the two will definitely improve the results. However, the challenge with this is that the region has a sparse station network and therefore data is not adequate. There is need for policy makers in the region to set aside adequate financial resources to be used in carrying out a station mapping exercise to identify areas to build new ones in accordance with the World Meteorological Organization (WMO) recommended standards.

A similar study should be undertaken for other weather parameters such as temperature, wind and moisture for the whole Greater Horn of Africa region in order to get the overall performance of the multimodel superensemble. Further, there is need to extend the range of forecasts to seasonal scale and beyond.

A further detailed study on the factors that influence weather over the GHA region

should be carried out in order to understand all the systems. This would lead to discovery of better forecasting techniques. The physics and the configuration of the regional models should in future consider factoring in the unique features that characterize the region.

Finally, IGAD Climate Prediction and Application Centre, being the focal point at the region should be enhanced especially in terms of computing facilities. This will enable the Centre to adopt current and emerging forecasting technologies.

REFERENCES

Anthes, R.A. (1983). Regional models of the atmosphere in middle latitudes. *Mon. Wea. Rev.,* **111**, 1306-1330.

Anyah, R. O., and Semazzi, F. H. M. (2007). Variability of East African rainfall based on multi-year RegCM3 model simulations. *International Journal of Climatology:* **27**, 357-371.

Anyamba, E.K. (1992). Some properties of a 20–30 day oscillation in tropical convection. J Afr Meteorol Soc **1**:1–19

Aonashi, K. (1993). An initialization method to incorporate precipitation data into a mesoscale numerical weather prediction model. *J. Meteor. Soc. Japan*, **71,** 393–406.

Asnani, G.C. (1993). The climate of Africa including feasibility study of climate alert system. *Proc. Techn. Conf. on climate-Africa*, 25-30

Bosire, E.N. (2012). Assessment of the predictability of rainfall on seasonal timescales over east Africa using the Forecast System Model, MSC Thesis, *Dept. of Meteorology, university of Nairobi*

Bowden, J. H., (2004). Recent and Projected Climate Variability during the Seasonal Rains of the Greater Horn of Africa. *MSc. Thesis, Marine, Earth,and Atmospheric Science, North Carolina State University,* 213 pp.

Brankovic, C. and Palmer, T.N. (1997). Atmospheric seasonal predictability and estimates of ensemble size. *Mon. Wea. Rev*. **125**, 859-874.

Buizza, R. (1998). Aspects of the performance of the ECMWF Ensemble Prediction System during winter 1996/97. Proceedings of the *1997 Expert Meeting on Ensemble Prediction*, ECMWF, Reading, U.K, 15-16 June 1998, 11-29.

Calvetti L., Filho A.J.P. (2014). Ensemble Hydrometeorological Forecasts Using WRF Hourly QPF and TopModel for a Middle Watershed. *Advances in Meteorology* **2014**, 1-12.

Chakraborty A., Krishnamurti, T. N, Mishra, A. K., and Rajeevan, M. (2009). Improving global model precipitation forecasts over India using downscaling and the FSU superensemble. Part I: 1–5-day forecasts. *Mon. Wea. Rev*., **137**, 2713–2735

Chakraborty, Arindam, Krishnamurti, T. N. (2006). Improved Seasonal Climate Forecasts of the South Asian Summer Monsoon Using a Suite of 13 Coupled Ocean–Atmosphere Models. *Mon. Wea. Rev.*, **134**, 1697–1721.

Chaves R.R., Mishra A.K., Krishnamurti T.N. (2005). Seasonal climate prediction for South America with FSU multi-model synthetic superensemble algorithm. *Meteorology and Atmospheric Physics **89**: 37–56.* Doi: http://dx.doi.org/10.1175//2571.1

Doblas-Reyes, F.J., D'equ'e, M. and Piedelievre, J.P. (2000). Multi-model spread and probabilistic forecasts in PROVOST.Q.J.R *Meteorol. Soc.* **126**, 2069-2087

Dong, S.W. (2001). Short to medium range superensemble precipitation forecasts using satellite derived products, PHD Dissertation, Department of Meteorology,Florida State University

Donner, L. J., Charles J. S., and Richard S. H. (1999). Ice microphysics and radiative transfer in deep convective systems In *10th Conference on Atmospheric Radiation*, 28 June-2 July 1999, Madison, WI, *American Meteorological Society*, 611-614.

F, E.K. (1992). Some properties of a 20-30 day oscillation in tropical convection. *African Meteorological Society.* **1**, 1-19.

Ferraro, R. R., Weng, F., Grody, N. C., and Basist, A. (1996). An eight-year (1987-1994) time series of rainfall, clouds, water vapor, snow cover, and sea ice derived from SSM/I measurements. *Bulletin of the American Meteorological Society*, **77,** 891-905.

Folland C.K., Owen, J., Ward, N., Colman, A. (1991). Prediction of seasonal rainfall in the Sahel region using empirical and dynamical methods. *Journal of forecasting*, **10**, p.21-56.

Gitutu J.M. (2006). A comparative verification of precipitation forecasts for selected

Numerical weather prediction models over Kenya. MSc.Dissertation, Dept. of Meteorology, University of Nairobi.

Goerss, J.S. (2000). Tropical cyclone track forecasts using an ensemble of dynamical models. *Mon. Wea. Rev.*, **128**, 1187-1193.

Graham, R.J., Mylne, A.D.L., Harrison, K.R., and Robertson K.B. (2000). An assessment of seasonal predictability using atmospheric general circulation models. *Q.J.R. Meteorol. Soc*. **126**, 2211-2240.

Heckley, W.A., Kelly, G., and Tiedtke, M. (1990). Sensitivity of ECMWF analyses-forecasts of Tropical Cyclones to cumulus parameterization. *Mon. Wea. Rev*. **118**, 1743-1757

Indeje, M., and Semazzi F. (2000). Relationships between QBO in the lower Equatorial Stratospheric Zonal Winds and East African Seasonal Rainfall. *J. Meteorol. Atmos. Phys.* **23**,227-244.

Indeje, M., Semazzi F.H.M., and Ogallo L.J. (2000). Enso signals in East African rainfall seasons. *Int. J. Climatol.,* **1,** 19-46

Ininda, J. (2008). Towards Improvement of seasonal rainfall forecasting through model output statistics (MOS) and downscaling of ECHAM Forecasts over Tanzania. ***J.*** *Kenya Meteorol. Soc.,* **2** (2), 96-104.

Jury, M.R., Pathack, B., and Parker, B. (1999). Climatic determinants and statistical prediction of tropical cyclone days in the Southwest Indian Ocean. *J Climate,* **12,** 1738-1746.

Kamga, A., Fongang, S., and Viltard, A. (2000). Systematic errors of the ECMWF operational model over tropical Africa. *Mon. Wea. Rev*, **128,** 1949–1959.

Kasahara, A., Mizze, A. P., and Donner, L. J. (1994). Diabatic initialization for improvement in the tropical analysis of divergence and moisture using satellite radiometric imagery data. *Tellus*, **46A,** 242–264.

Kharin, V. V., and Zwiers, F. W. (2002). Notes and correspondence; Climate predictions with multi-model ensembles. *J. Climate*, **15**, 793-799.

Kibara, D.G., (2011). Predictabity of weather on extended NWP time scales over Kenya using the NCEP GFS model, MSC Thesis, Dept. of Meteorology, University of Nairobi.

Kirtman, B.P., Huang B., Zhu, Z., and Scheider, E.K. (1997). Multiseasonal predictions with a coupled tropical ocean global atmosphere system. *Mon. Wea. Rev.,* **125**, 789-808**.**

Kirtman, B.P., Min, D., Schopf, P.S., and Scheider, E.K. (2003). A new approach for coupled GCM sensitivity studies. COLA Technical Report CTR **154**, 48pp.

Krishnamurti T.N., Bachiochi D., LaRow T., Jha B., Tewari M., Chakraborty D.R., Torres R.J.C., Oosterhof D. (2000b). Coupled atmosphere-ocean modeling of El-Nino of 1997–98. *Journal of Climate* **13***:* 2428–2459.

Krishnamurti T.N., Kishtawal C.M., Zhang Z., LaRow T., Bachiochi D., Williford E., Gadgil S., Surendran S. (2000a). Multi-model ensemble forecasts for weather and seasonal climate. Journal of Climate 13*:* 4196–4216.

Krishnamurti, T. N., Rajendran K., Kumar T. S. V., Lord S., Toth, Z., Zou, X., Cocke, S., Jon E., Ahlquist, I., and Navon., M. (2003). Improved Skill for the Anomaly Correlation of Geo-potential Heights at 500 hPa. *Monthly Weather Review* **131**:6, 1082-1102

Krishnamurti, T. N., Bedi, H. S., Ingles, K., Heckley, W., and Ingles, K. (1988). Reduction of the spin-up time for evaporation and precipitation in a spectral model. *Mon. Wea. Rev.*, **116,** 907–920.

Krishnamurti, T. N., Chakraborty, D. R. (2005). The Dynamics of Phase Locking. *J. Atmos. Sci.*, **62**, 2952–2964. doi: http://dx.doi.org/10.1175/JAS3507.1

Krishnamurti, T. N., Gnanaseelan, C., Mishra, A.K., and Chakraborty, A. (2008). Improved forecasts of diurnal cycle in tropics using multiple global models. Part 1: *Precipitation. J. Climate,* **21**, 4029-4043.

Krishnamurti, T. N., Ingles, K., Cocke, S., Pasch, R., and Kitade, T. (1984). Details of low latitude medium range numerical weather prediction using a global spectral model. II. Effect of orography and physical initialization. *J. Meteor. Soc. Japan*,

62, 613–649.

Krishnamurti, T. N., Kishtawal, C. M., LaRow, T. E., Bachiochi, D. R., Zhang, Z., Williford, C. E., Gadgil, S., and Surendran, S. (1999). Improved weather and seasonal climate forecasts from multimodel superensemble. *Science*, **285**, 1548–1550.

Krishnamurti, T. N., Kumar, V. (2012): Improved Seasonal Precipitation Forecasts for the Asian Monsoon Using 16 Atmosphere–Ocean Coupled Models. Part II: Anomaly. *J. Climate*, **25**, 65–88. doi: http://dx.doi.org/10.1175/2011JCLI4126.1

Krishnamurti, T. N., Pattnaik, S., Stefanova, L., Kumar, T. S. V., Mackey, B. P., O'Shay, A. J,. Pasch. R. J. (2005). The Hurricane Intensity Issue. *Monthly Weather Review* **133**:7, 1886-1912

Krishnamurti, T. N., Surendran, S., Shin, D. W., Correa-Torres, R. J., Kumar, T. S. V.,Williford, C. E., Kummerow, C., Adler, R. F., Simpson, J., Kakar, R., Olson, W.S., and Turk, F. J. (2001). Real time multi-analysis/multi-model superensemble forecasts of precipitation using TRMM and SSM/I products. *Mon. Wea. Rev.,* **129**, 2861-1883.

Krishnamurti, T. N., Xue, J., Bedi, H. S., Ingles, K., and Oosterhof, D. (1991). Physical initialization for numerical weather prediction over the tropics. *Tellus*, **43AB,** 53–81.

Krishnamurti, T.N., Bedi, H., Rohaly, G., and Oosterof, D. (1996). Partitioning of the seasonal simulation of a monsoon climate. *Mon. Wea. Rev*., **124**, 1499-1520.

Krishnamurti, T.N., Stefanova, L., Chakraborty A., Kumar T.S.V., Cocke S., Bachiochi D., Mackey B. (2002). Seasonal Forecasts of Precipitation Anomalies for North American and Asian Monsoons.. *Journal of the Meteorological Society of Japan* **80**:6, 1415-1426

Kummerow, C., and co-authors. (2000). The status of the Tropical Rainfall Measuring Mission (TRMM) after two years in orbit. *J. Appl. Meteor. ,* **39**, 1965–1982.

Kummerow, C., Olson, W.S., and Giglio, L. (1996). A simplified scheme for obtaining precipitation and vertical hydrometeor profiles from passive microwave sensors. *IEEE Trans. On Geosci. And Remote Sensing*, **34**, 1213-1232.

Latif, M., Sperber K., Arblaster J., Braconnot P., Chen D., Colman A., Cubasch U., Cooper C., Delecluse P., De Witt D., Fairhead L., Flato G., Hogan T., Ji M., Kimoto M., Kitoh A., Knutson T., Le Treut H., Li T., Manabe, S., Marti, O., Mechoso C., Meehl G., Roeckner E., Sirven J., Terray L., Vintzileos, A., Wang, B., Washington, W., Yoshikawa, I., Yu, J. and Zebiak S. (2001). The El Nino simulation inter-comparison project (ENSIP). *Clim Dyn.,* **18,** 255–276.

Lee, S., Haksu, Z., Zhang, Y.,Dong, J.S., Robert J., Kuligowski, G., Kitzmiller, D., and Corby, R. (2014). Utility of SCaMPR Satellite versus Ground-Based Quantitative Precipitation Estimates in Operational Flood Forecasting: The Effects of TRMM Data Ingest. *J. Hydrometeor*, **15**, 1051–1069.

Mishra A.K., and Krishnamurti, T.N. (2007). Current Status of multi-model Superensemble and operational NWP forecast of the Indian summer monsoon. Journal of Earth System Science, **116**(5), 369-384

Molteni, F., Buizza, R., Palmer, T.N., and Petroliagis, T. (1996). The ECMWF ensemble prediction system: Methodology and validation. *Q.J.R Meteorol. Soc*. **122**, 73-119.

Mukabana, J. R. (1992). Numerical simulation of the influence of the large scale monsoon flow on the weather patterns over Kenya using a three dimensional limited area model. *PhD Thesis, University of Nairobi.*

Mukabana, J.R., and Pielke, R.A. (1996). Investigating the influence of synoptic-scale monsoonal winds and mesoscale circulations on diurnal weather patterns over Kenya using a mesoscale numerical model. *Mon. Wea. Rev*., **124**, 224-243.

Mutai, C. C., and Ward, M.N. (2000). East African rainfall and the tropical circulation convection on intraseasonal to interannual time scales. *J. Climate,* **3,** 3915–3939.

Mutai, C.C., Ward, M.N., and Coleman, A.W. (1998). Towards the prediction of the East Africa short rains based on sea-surface.

Mutemi, J. N. (2003). Climate anomalies over East Africa associated with various ENSO evolution Phases. PhD Thesis, *University of Nairobi*.

Mutemi, J.N., Ogallo L.A., Krishnamurti T.N., Mishra A.K., Kumar V.T.S.V. (2007). Multi-model based superensemble forecasts for short and medium range NWP over various regions of Africa. *Meteorology and Atmospheric Physics,* **95**:1-2, 87-113

Nicholson, S. E. (2014). The Predictability of Rainfall over the Greater Horn of Africa. Part I: Prediction of Seasonal Rainfall. *J. Hydrometeor*, ***15*(3)**, 1011–1027.

Ogallo, L. (1979). Rainfall Variability in Africa. *Mon. Wea. Rev.*, **107**, 1133–1139.

Ogallo, L. A. (1989). The spatial and temporal patterns of East African seasonal rainfall derived from principal component analysis; *Int. J. Climatol.,* **9,** 145–167.

Ogallo, L.J. (1988). Relationships between seasonal rainfall in East Africa and the Southern Oscillation, *J. Climatol*., **8**, 31–43.

Okoola, R., Camberlin, P., and Ininda, J., M. (2008). Wet periods along the East Africa Coast and the extreme wet spell event of October 1997**.** *J. Kenya Meteorol. Soc.***,** **2**(1) 65–81.

Omeny, P., Ogallo, L., and Okoola, R. (2008). East Africa rainfall variability associated with the MJO, J. *Kenya Meteorol. Soc*., **2**, 105–114.

Omondi, P., Ogallo L., and Okoola, R. (2009). Decadal Rainfall Variability Modes in observed Rainfall Records over East Africa and their Predictability using Sea Surface Temperature **.***J.Meteorol. Rel. Sci.,* **3**, 37–54.

Omondi, P.A. (2010). Teleconnections between decadal rainfall variability and global sea surface temperatures and simulation of future climate scenarios over East Africa, *PHD Thesis, Dept. of Meteorology, University of Nairobi.*

Palmer, T.N., Alessandri, A., Andersen, U., Cantalaube, P., Davey, M., and co-authors. (2004). Development of a European multi-model ensemble system for seasonal to interannual prediction (DEMETER). *Bull. Am. Meteorol. Soc.* **85**, 853-872.

Palmer, T.N., Alessandri, A., Andersen, U., Cantelaube, P., Davey, M., and co-authors. (2003). Development of a European multimodel ensemble system for seasonal to interannual prediction (DEMETER). *Bull. Am. Meteorol. Soc.* **85**, 853-872.

Palmer, T.N., Brankovic, C., and Richardson, D.S. (2000). A probability and decision model analysis of PROVOST seasonal multi-model ensemble integration. *Q.J.R Meteorol. Soc.* **126**, 2013-2034.

Peng, P., Kumar, A., Van den Dool, A.H., and Barnston, A.G. (2002). Analysis of multi-model ensemble predictions for seasonal climate anomalies. *J. Geophys. Res*. **107**, 4710 (doi:10.1029/2002JD002712)

Puri, K., and Davidson, N. E. (1992). The use of infrared satellite cloud imagery as proxy data for moisture and diabatic heating in data assimilation. *Mon. Wea. Rev.*, **120,** 2329–2341.

Puri, K., and Miller, M. J. (1990). The use of satellite data in the specification of convective heating for diabatic initialization and moisture adjustment in numerical weather prediction models. *Mon. Wea. Rev.*, **118,** 67–93.

Rajeeyan, M., Pai, D.S., Dikshit, S.K., and Kelkar, R.R. (2006). IMD's new operational models for long range forecast of Southwest monsoon rainfall over India and their verification for 2003. *Curr. Sci.,* **86**, 422-431

Ross R.S., Krishnamurti T.N., (2005). Reduction of forecast error for global numerical weather prediction by the Florida State University (FSU) Superensemble. *Meteorol Atmos Phys* **88**: 215–235

Sakwa V.N. (2006). Assessment of the skill of the High Resolution Regional Model in the simulation of airflow and rainfall over East Africa. *Msc.dissertation, Dept. of Meteorology, University of Nairobi.*

Schaefer, J. T., (1990). "The critical success index as an indicator of warning skill". *Wea. Forecasting*, **5**, 570-575.

Schreck, C.J. and Semazzi F.H.M. (2004). Variability of the recent climate of eastern Africa. *Int. J. Climatol.,* **24**, 681-701

Stefanova, L., and Krishnamurti, T. N. (2002). Interpretation of Seasonal Climate Forecast Using Brier Skill Score, The Florida State University Superensemble, and the AMIP-I Dataset. *J. Climate*, **15**, 537-544.

Strauss, D. M., and Shukla, J. (2000). Distinguishing between the SST forced variability and internal variability in mid-latitudes: Analysis of observations and GCM simulation *Quart.J. Roy. Meteor. Soc.,* **126**, 2323-2350.

Toth, Z., and E. Kalnay, (1993). Ensemble forecasting at NMC: The perturbations. *Bull. Amer. Meteor. Soc.,* **74**, 2317-2330.

Toth, Z., and Kalnay, E. (1997). Ensemble forecasting at NCEP and the breeding method. *Mon. Wea. Rev.,* **125**, 3297-3319.

Treadon, R. E. (1996). Physical initialization in the NMC global data assimilation system. *Meteor. Atmos. Phys.*, **60,** 57–86.

Veenhuis, B.A. (2013). Spread Calibration of Ensemble MOS Forecasts. *Monthly Weather Review,* **141**:7, 2467-2482.

Webster, P.J., Magana, V.O., Palmer, T.N., Shukla, J., Tomas, R.A., Yanai,M., and Yasunari, T. (1998). Monsoons: Processes, predictability, and the prospects for prediction. *J. Geophys. Res.-Oceans,* **103**, 14451-14510.

Wilks, D.S. (1995). Statistical methods in the atmospheric sciences. *New York. Academic Press*, 467 pp

Williford, C.E., Krishnamurti T.N., Torres, R.C., Cocke, T. (2003). Real-time multimodel superensemble forecasts of Atlantic tropical systems of 1999. *Mon Wea Rev* **131**:1878–1894

Williford, E. C., Krishnamurti, T. N., Torres, R.C., Zaphiris, S.C.C., Kumar, T. S. V. (2003). Real-Time Multimodel Superensemble Forecasts of Atlantic Tropical Systems of 1999. *Mon. Wea. Rev.*, **131**, 1878–1894.

Yun, W.T., Stefanova, L., and Krishnamurti, T. N. (2003). Improvement of the multi-model superensemble technique for seasonal forecasts. *J. Climate*, **16**, 3834-3840.

Zwiers, F.W. (1996). Interannual variability and predictability in an ensemble of AMIP climate simulations conducted with the CCC GCM2. *Climate Dyn.,* **12**, 825-847.